Available online at www.sciencedirect.com
SCIENCE DIRECT®
Journal of Photochemistry and Photobiology C: Photochemistry Reviews
4 (2003) 155–177
Journal of Photochemistry and Photobiology C: Photochemistry Reviews
www.elsevier.com/locate/jphotochemrev

Review

Computational methods for electron-transfer systems

Ata Amini, Anthony Harriman*

Molecular Photonics Laboratory, School of Natural Sciences (Chemistry), University of Newcastle, Bedson Building, Newcastle upon Tyne NE1 7RU, UK

Received 1 June 2003; received in revised form 8 July 2003; accepted 8 July 2003

Abstract

Electron-transfer processes, and especially light-induced electron-transfer reactions, play an extremely important role in natural and artificial energy transduction. Following many decades of intensive theoretical and experimental study, it is now opportune to explore electron-transfer processes by way of modern computational chemistry. In essence, this requires the meaningful calculation of those thermodynamic parameters that combine to control the rate of electron-transfer between remote donor and acceptor species. The most important parameters are the nuclear and solvent re-organisation energies, the electronic coupling matrix element, the change in Gibbs free-energy and the activation energy change accompanying electron-transfer. Clearly, the surrounding environment has to be taken into account. Restricting attention to intramolecular electron-transfer in tripartite supermolecules of general type donor–bridge–acceptor (D–B–A), it is possible to compute each of the required thermodynamic properties from first principles. We examine here the most common quantum chemical approaches for estimation of each term and show that it is possible to arrive at a realistic estimate of the overall rate of electron-transfer. Attention is focused on readily accessible computational methodology.

Keywords: Quantum chemistry; Computational chemistry; Coupling element; Electron-transfer; Re-organisation energy; Free-energy change; Activation energy; Charge transfer; Electronic coupling matrix element

Contents

* Corresponding author. Fax: +44-191-222-8660.
E-mail address: anthony.harriman@ncl.ac.uk (A. Harriman).

1389-5567/$ 20.00
doi:10.1016/S1389-5567(03)00027-3

1. Introduction

Electron-transfer is a fundamental process that underpins most of the biological, chemical, and physical systems concerned with the production and/or storage of energy. Such reactions are particularly prevalent in photochemistry and photobiology, most notably in the natural photosynthetic process. Light-induced electron-transfer reactions have been studied in detail for more than 50 years and many important mechanistic details have been brought to the surface. In part, the success of this work stems from the availability of appropriate experimental tools, such as laser flash photolysis and time-resolved fluorescence spectroscopy, that can follow the fate of the reaction intermediates over variable time scales. Indeed, laser flash photolysis, together with pulse radiolysis, has provided the experimental support by which to develop sophisticated theoretical models for explaining the rate of electron-transfer in many different environments. Because of such studies, carried out by innumerable research groups, we now know most of the factors that combine to control the rate of electron-transfer. This information has been used to design and synthesise elaborate supermolecules able to achieve a cascade of electron-transfer steps covering many tens of Ångstroms. In turn, such systems are being used to create light-activated molecular machines and it seems inevitable that molecular-scale photoelectronic devices will soon be on the market.

The last few years have seen new developments in the study of electron-transfer reactions. In particular, there has been a tremendous growth in the application of modern computational methods to the study of electron and charge transfer in chemical and biological systems. These studies have been fuelled by the availability of sophisticated software and fast computers. It is now possible to examine putative electron-transfer reactions entirely by quantum chemical methods and to compute meaningful values for the various thermodynamic parameters associated with charge transfer. Agreement between theory and experiment is converging and it has to be admitted that the computational approaches can provide deep insight into the mechanism of the electron-transfer step. Such realisations mean that it will soon be possible to set-up the quantum chemical equivalent of combinatorial chemistry. That is to say, rather than synthesise new molecules and determine rates of electron-transfer it will be possible to first study the system by computational approaches and identify the most appropriate subunits for the task at hand. This is the only way forward if we are to successfully design molecular-scale photoelectronic devices since the alternative approach of synthesising numerous series of multi-component supermolecules is far too time-consuming. In this review, we examine the various computational methods that are currently available for studying electron-transfer processes.

Most systems undergo some kind of structural change during electron-transfer [1–3], even for an intramolecular process occurring in a solid medium. This structural change can be considered in terms of a nuclear re-organisation energy that, in part, influences the rate of the electron-transfer step. Likewise, surrounding solvent molecules will re-orientate or rearrange around the solute during the electron-transfer step since the overall electronic charge must change; or, in a charge-shift reaction, the relative electron density will be redistributed. This leads to a further thermodynamic parameter, namely the solvent re-organisation energy, that also has to be accommodated in the overall rate equation. These two re-organisation energies are involved in the reaction co-ordinate for the potential energy curves drawn to simulate the course of an electron-transfer process. Let us refer to this co-ordinate as q, and with the reactants and products specified as R and P, respectively. The potential energy curves for the reactants and products are dependent on this reaction co-ordinate as follows [4–7]:

$$V_R = \tfrac{1}{2}k(q + q_0)^2 \quad (1)$$

$$V_P = \tfrac{1}{2}k(q - q_0)^2 \quad (2)$$

Here, k is the force constant and q_0 is the value of q at the minimum point on the potential energy surface (PES). The difference between these two energies is as follows:

$$V_R - V_P = 2kq_0q \quad (3)$$

This expression indicates that the potential energy difference is directly proportional to the reaction co-ordinate [8–10]. Thus, for a system comprising an electron donor, D, connected to an electron acceptor, A, via a bridge, B (i.e. donor–bridge–acceptor or D–B–A), the V_R and V_P refer to D–B–A and D^+BA^-, respectively, and are expected to display a parabolic function with respect to the reaction co-ordinate ($V_R - V_P$), as illustrated in Fig. 1. The first part of this study is devoted to investigating the available theoretical approaches that could be used to construct the relevant potential energy curves. This is a critical component

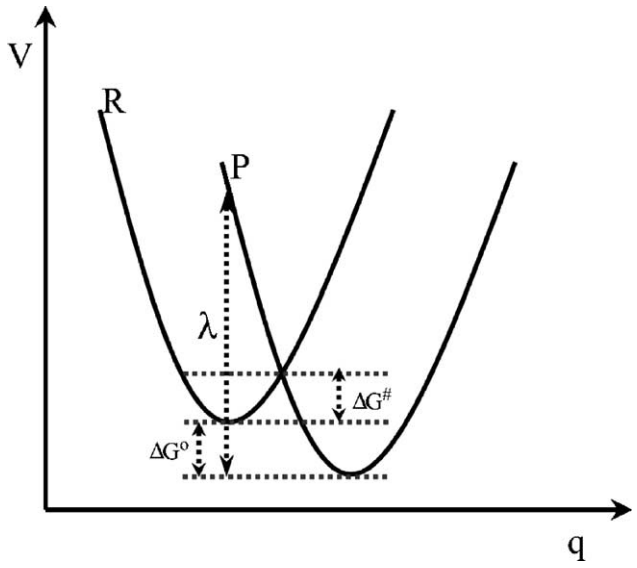

Fig. 1. Representation of the parabolic free-energy curves for the reactants (R) and products (P) of a typical electron-transfer reaction.

of the overall strategy for using quantum chemistry to compute rates of electron-transfer.

It is well established that the rate of electron-transfer (k_{ET}) shows an exponential dependence on the activation energy ($\Delta G^{\#}$) for electron-transfer, according to the following expression [8–10]:

$$k_{ET} = A e^{-\Delta G^{\#}/k_B T} \quad (4)$$

Here, A and k_B are the pre-exponential factor and the Boltzmann constant, respectively. It has to be realised that this simple relationship holds providing the rate of electron-transfer can be properly separated from physical processes such as diffusion. This is best done by studying intramolecular electron-transfer or by restricting attention to electron-transfer processes occurring in a rigid environment. Under such conditions, $\Delta G^{\#}$ is related to the re-organisation energy (λ) and the change in reaction free-energy (ΔG°) as follows:

$$\Delta G^{\#} = \frac{(\lambda + \Delta G^{\circ})^2}{4\lambda} \quad (5)$$

Here,

$$\lambda = \lambda_S + \lambda_N \quad (6)$$

where λ_N and λ_S, respectively, are the nuclear and solvent re-organisation energies. According to this approach, in order to compute the rate of electron-transfer, it is first necessary to calculate appropriate values for λ_N, λ_S, and ΔG°. Each of these parameters requires special considerations and, as a consequence, they are treated separately in the following discussion.

Electron-transfer reactions may be classified in terms of the mutual interactions between the electronic states R and P as being adiabatic or non-adiabatic [6,10,11]. In the latter type of reactions, the electronic coupling matrix element describing interaction between D and A is very weak (i.e. D and A are well separated in electronic, in not spatial, terms) and the rate expression can be considered in terms of the Fermi Golden rule [6,10,11]. According to this expression, the rate constant is proportional to the Franck–Condon weighted-density (FCWD) of states and the electronic coupling matrix element (H_{RP}) as follows [6]:

$$k_{ET} = \frac{2\pi}{\hbar} H_{RP}^2 (\text{FCWD}) \quad (7)$$

It is extremely difficult to determine the size of the coupling element in most experimental studies, except in certain special cases, unless a mechanism is assumed and all other parameters are measured separately. However, several methods exist by which to compute the coupling element and, in the final section of this article, we review the computational approaches available for calculation of the coupling elements for various types of different molecular systems.

2. Potential energy surfaces (free-energy curves)

A PES can be considered to be a pathway that links reactant with product and that facilitates examination of whether-or-not a particular reaction is feasible on this given pathway. For a diatomic molecule, this surface could be a two-dimensional curve of potential energy versus bond distance. However, for an N nuclei non-linear or linear system, the PES has $3N - 5$ and $3N - 4$ dimensions, respectively. Generally, a reaction path along the PES contains an energy minimum corresponding to the reactant state, a barrier of a particular height and shape, and a second valley corresponding to the product state. More often than not, other minima appear on the PES and can be assigned to the involvement of metastable intermediate species. A variety of important points can be recognised along the PES as the reactant state evolves towards the product state; these include local minima, local maxima, saddle points and transition state structures that are usually referred to as stationary points. The first and second derivatives of the potential energy (i.e. gradient and Hessian, respectively) calculated with respect to these variables can be used to determine the precise location on any PES. For local minima, all of the eigenvalues of the Hessian point are positive while for the corresponding maxima all of the eigenvalues are negative. Saddle points have just one negative eigenvalue with the rest being positive, but transition states have more than one negative eigenvalue.

Molecular orbital (MO) methods provide the most commonly used approaches for calculating these curves theoretically, although the valence bond structure method has certain advantages in some instances as will be discussed in the following section. Molecular dynamics (MD) simulations can also be exploited in order to simulate the effect of solvent molecules on the energy of the electron-transfer

system under examination. This situation can be used to estimate reaction free-energy curves. In turn, the latter curves can be used to compute the required thermodynamic parameters associated with the electron-transfer event. In reality, it is usually necessary to use a combination of computational methods in order to fully examine the overall system.

2.1. Empirical valence bond (EVB) method

It is widely recognised that the nature of the environment often exerts a significant influence on the rates, and indeed the mechanisms, of those chemical reactions that involve bond breaking or making and that pass through an ionic transition state. The empirical valence bond (EVB) method is a well-established approach for finding the potential energy curves [12,13] of such reactions as the nature of the surrounding medium changes. For example, consider a reaction in which the X–Y state (ψ_1) is neutral but can be converted into either the X^-X^+ state (ψ_2) or the analogous X^+Y^- state (ψ_3). The secular equation for the system in the gas phase can be written as follows:

$$\begin{vmatrix} H_{11}^{g} - E^{g} & H_{12}^{g} - E^{g}S_{12} \\ H_{21}^{g} - E^{g}S_{21} & H_{22}^{g} - E^{g} \end{vmatrix} = 0 \tag{8}$$

The diagonal term for the neutral state can be found using the Morse-type potential function:

$$H_{11}^{g} = E_1^{g} = D\left[e^{-2a(r-r_0)} - 2e^{-a(r-r_0)}\right] \tag{9}$$

where r and r_0 are the X–Y bond length and the gas-phase equilibrium bond length, respectively, and a is found from the stretching vibrational frequency. The value of the bond dissociation energy (D) is calculated from the individual bond energies according to the following equation [14–16]:

$$D = \sqrt{D_{XX}D_{YY}} \tag{10}$$

The energy of the diagonal term of the ionised state can be found as follows:

$$E_1^{g} = \Delta^{(2)} - \frac{e^2}{r} + V_{nb}^{(2)} \tag{11}$$

where $\Delta^{(2)} = I_{(Y)} - E_{A(X)}$, with E_A and I refer to the electron affinity of the electron acceptor and the ionisation potential of the donor, respectively, and V_{nb} is the non-bonded potential function.

The off-diagonal terms can be found from the following equation:

$$H_{12}^{g} = \sqrt{(E_1^{g} - M_{XY})(E_2^{g} - M_{XY})} \tag{12}$$

Here, M is the Morse potential:

$$M = D[e^{-2a(r-r_0)} - 2e^{-a(r-r_0)}] \tag{13}$$

If we transfer the system from vacuum to solution, the energy of the initial neutral state will be unchanged but that of the final ionic state is changed by a factor corresponding to the solvation free-energy (G_{sol}):

$$\begin{aligned} E_1^{s} &= E_1^{g} \\ E_2^{s} &= E_2^{g} + G_{sol} \end{aligned} \tag{14}$$

Diagonalising the secular determinant for the above system in solution gives the energies of the ground state and excited state surfaces as follows:

$$E_{\pm} = \tfrac{1}{2}[(E_1^{s} + E_2^{s}) \pm \sqrt{(E_1^{s} - E_2^{s})^2 - 4(H_{12})^2}] \tag{15}$$

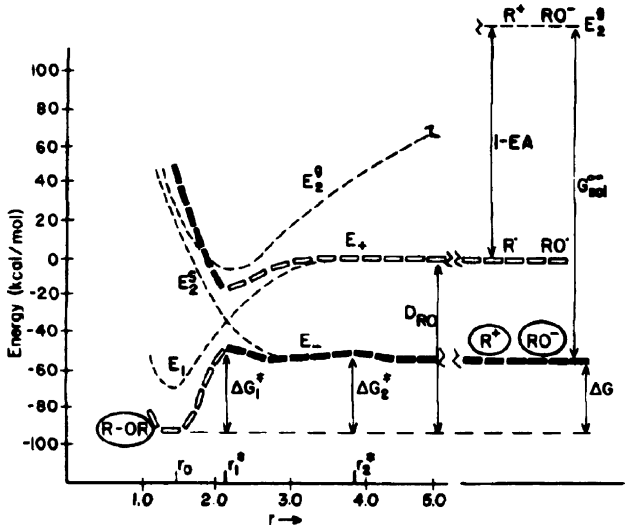

Fig. 2. The results of calculation for ionic bond cleavage in solution for the reaction R–O–R′ → $R^+ + R'O^-$ (see [12] for details).

Fig. 2 shows an example of the relevant PESs associated with the heterocyclic cleavage of the glycoside bond of a disaccharide [12]. The method has been used extensively in the literature; for example in calculating the free-energy curves for the staphylococcal nuclease [17] and for the free-energy curves that describe the general effects caused by replacement of Ca^{2+} with other cations [18].

2.2. A microscopic molecular dynamics treatment

The dynamical fluctuations of a system undergoing electron-transfer can be monitored using MD simulations in such as way as to extract those thermodynamic parameters related to the rate of electron-transfer by classical Marcus theory [8–10]. To do this, we need to consider two PESs for the system; one PES refers to the initial state prior to electron-transfer where the electron is localised on the donor and the second PES refers to the final system after electron-transfer where the electron has moved to the acceptor. These two states can be designated as $D–A^+$ and $D^+–A$, respectively. The potential energy of the system on each of these two surfaces is a combination of internal energy, electrostatic interactions between solvent molecules and solute, and any interactions between solvent molecules (V_I and V_{II}). Fluctuations along the solvent co-ordinate change

the potential energy of the system on both surfaces. But, there is a point on the surfaces where the potential energies are identical. This situation becomes apparent by following the potential energy difference ($V_{II} - V_I$) as a function of time, this being equivalent to the reaction co-ordinate [4]. The potential energy difference at any specific time can be found from analysis of the classical trajectories. The energy gap fluctuates with time, but the system reaches a condition where the energy gap is small and the probability of transfer of an electron from donor to acceptor is increased. The probability of reaching the intersection area is equal to $\exp[(-\Delta V_1^{\#})/k_B T]$, where $\Delta V_I^{\#}$ is the energy difference on the PES I in the intersection area. The probability can then be defined in terms of the free-energy change and can be calculated using the following equation:

$$\Delta G_1^{\#}(\theta^{\#}) = -k_B T \ln\{n(\theta^{\#})/n(\theta_1^{\circ})\} \quad (16)$$

Here, θ is the reaction co-ordinate, ΔG the free-energy change, and n is the number of times that the two PESs intersect (as calculated from MD trajectories). The free-energy curves for a typical system are shown in Fig. 3. It is apparent that these curves could be used to calculate values for the re-organisation energy and the activation free-energy change for electron-transfer.

The method has been extensively developed and tested by several research groups, mainly Warshel and co-workers [12,17–27] and Schulten and co-workers [28–30]. In particular, MD simulations have been used to derive re-organisation energies and activation free-energy changes for photosynthetic reaction centre complex. However, many other groups have utilised this approach for studying electron-transfer in model inorganic, organic and organometallic systems, including intermolecular electron-transfer between *N*,*N*-dimethylaniline and anthracene [31], intramolecular electron-transfer within porphyrin–benzoquinone dyads [32], electron-transfer between metal ions [33], electron exchange in aqueous Fe^{2+}–Fe^{3+} solution [34] and other systems [35].

The method as outlined briefly above can be used to calculate some of the important thermodynamic parameters necessary to compute the rate of electron-transfer. In the Marcus free-energy diagram [8,9], the energies of electron-transfer reaction products and reactants are dependent on the reaction co-ordinate as follows:

$$E_R(q) = \tfrac{1}{2}kq^2 \quad (17)$$

$$E_P(q) = \tfrac{1}{2}k(q - q_P)^2 - \Delta G^{\circ} \quad (18)$$

Here, k, q, and ΔG° are the force constant, reaction co-ordinate and reaction free-energy change, respectively. The energy difference between reactants and products may be written as

$$\Delta E(t) = kqq_P(t) + \Delta G^{\circ} - \tfrac{1}{2}kq_P^2 \quad (19)$$

This expression emphasises the fact that the relevant energy difference is directly proportional to the reaction co-ordinate. The term $\Delta E(t)$ can be calculated from MD simulation on two PESs with partial atomic charges of the reacting species in neutral and ionised forms. These latter forms must describe the system before (R) and after (P) electron-transfer. The partial charges of the reacting species in both initial and final states can be obtained from quantum mechanics calculations, whilst for the rest of the residues (e.g. the protein matrix) the default values available in software such as CHARMM are used [36]. The computation starts with a MD simulation on the equilibrated system with the reacting species in their neutral state. For each conformation of the system at a specific simulation time, the energy of the entire system is calculated in both electronic states. That is to say, the required energy gap is calculated for charge distributions corresponding to before and after electron-transfer:

$$\Delta E_R(t) = E_P(t) - E_R(t) \quad (20)$$

The same procedure is performed on the PES of the system but starting with ionised species (i.e. after electron-transfer), which gives:

$$\Delta E_P(t) = E_P(t) - E_R(t) \quad (21)$$

The re-organisation energy and the reaction free-energy change are now calculated from the average values of the energy differences as follows:

$$\lambda = \tfrac{1}{2}[\langle \Delta E \rangle_P - \langle \Delta E \rangle_R] = -\tfrac{1}{2}\Delta\Delta E \quad (22)$$

$$\Delta G^{\circ} = \tfrac{1}{2}[\langle \Delta E \rangle_P + \langle \Delta E \rangle_R] \quad (23)$$

Fig. 3 shows the free-energy difference from MD simulations for transfer of an electron from the special pair (P_s) to the nearby bacteriopheophytin (H_L) molecule in the bacterial photosynthetic reaction centre at a few different temperatures [21,22]. The method has been applied to the particular problem of electron-transfer in photosynthetic reaction centre complexes by several research groups [26–30,37] with spectacular success. The importance of this work is made even more obvious when considering the size and complexity of the protein system.

3. Nuclear re-organisation energy

Klimkans and Larsson [38] have developed a method that facilitates calculation of the nuclear re-organisation energy. This approach is illustrated schematically in Fig. 4. According to this method, the geometry of the molecule in its first electronic state [M(II)] is optimised with respect to energy, E_1. An electron is moved from the system so as to generate [M(III)] and the energy is re-calculated without any change in the geometry, E_2. Now, the structure of the molecule after electron-transfer is optimised to give the minimised energy, E_3. The system is then returned to its first position [M(II)] and the energy is re-calculated but with the geometry pertaining to the system after transfer of the electron, E_4. The

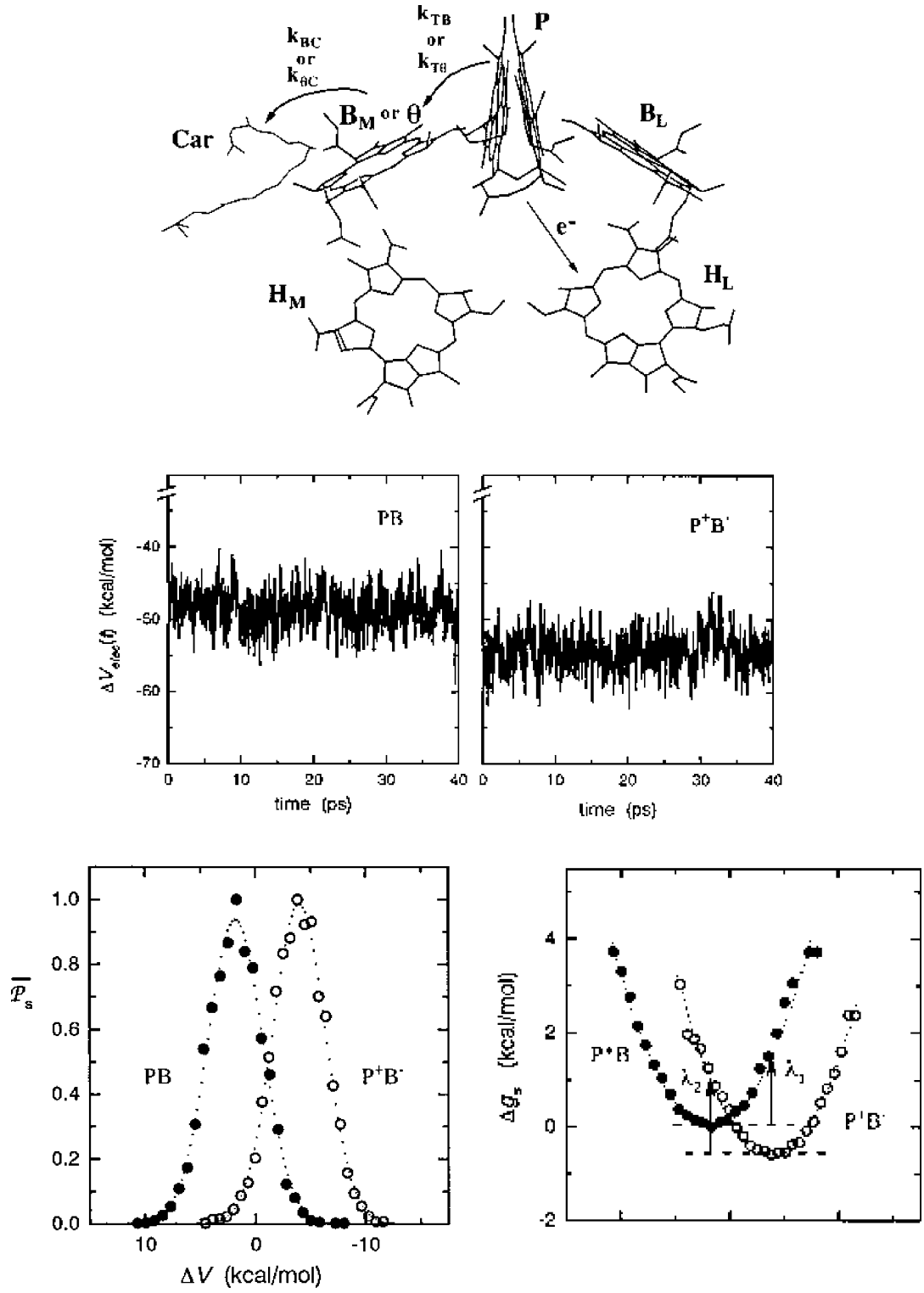

Fig. 3. An outline scheme showing the arrangement of the essential cofactors of the bacterial photosynthetic reaction centre complex as provided by X-ray crystal structural data (top). The time-dependent energy gap between PB and P^+B^- on both potential energy surfaces (centre). The probabilities for distributions of energy gaps and the free-energy curves for two electronic states corresponding to P*B and P^+B^- (bottom) (see [21] for details).

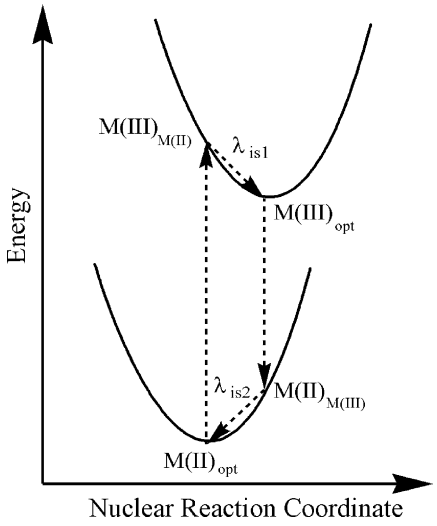

Fig. 4. Schematic representation of the theoretical method used for calculation of the nuclear re-organisation energy (see [38] for details).

nuclear re-organisation energy is calculated using the following equations:

$$\lambda_{N1} = E_2 - E_3$$
$$\lambda_{N2} = E_4 - E_1 \quad (24)$$
$$\lambda = \lambda_1 + \lambda_2$$

This approach has been modified and used extensively for a wide variety of organic and inorganic systems [38–46]. Fig. 4 illustrates in a schematic fashion how the nuclear re-organisation energy can be extracted from the various energy terms [39].

In the second method, the molecule is broken into two components; one fragment corresponds to the best estimate of the electron donor and the other fragment refers to the electron acceptor. Of course, it is not always obvious which parts of the molecule to take as being fully representative of the donor and acceptor. The best way to proceed is to make a series of MO computations to visualise the relevant orbitals on the LUMO and HOMO involved directly in the electron-transfer event. This approach helps to identify the main molecular fragments. Fig. 5 shows an example of a nuclear re-organisation energy calculation carried out by Kurnikov et al. [47] and others [48].

The first molecular fragment corresponds to D/D^+ whereas the second component can be considered to represent the A/A^- transformation. Taking the optimised structures of D and A as referring to the donor and acceptor before charge transfer and those of D^+ and A^- as being the electron-transfer products, an approximate value for λ_N can be computed as the sum of the re-organisation energies for the two individual components. Clearly, this simplified approach neglects any contributions caused by mutual interactions between donor and acceptor that might occur in a molecular dyad. However, the approach is inherently simple and provides a means for dealing with large and complicated systems.

Making use of the optimised structure for D, the energy is calculated for (E_{R1}) and the hypothetical D^+ having the same geometry as D (E_{R2}). The calculation is then repeated

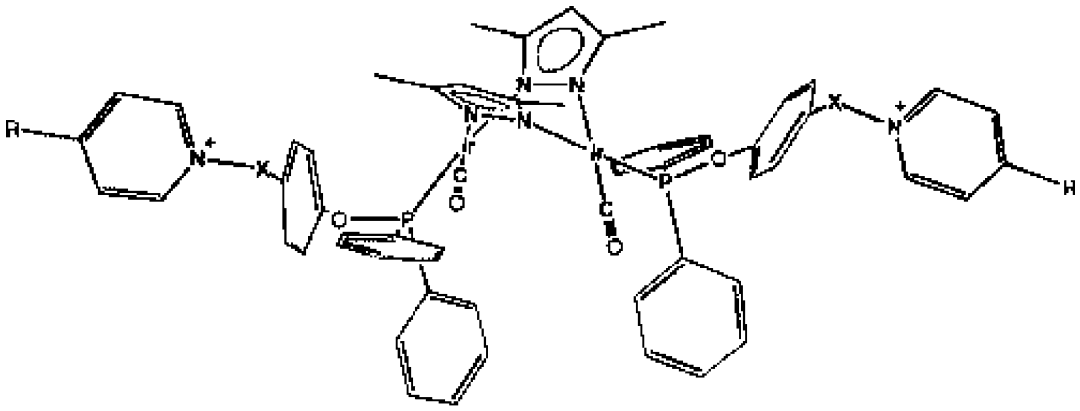

X = –	R = H	PC0
X = CH_2	R = H	PC1
X = CH_2	R = t-Bu	PC1-tBu
X = CH_2	R = Am	PC1-Am
X = $(CH_2)_2$	R = H	PC2
X = $(CH_2)_3$	R = H	PC3

Fig. 5. Structures of some molecular triads used in the FDPB calculations (see [47] for details).

but starting from the optimised structure for D^+ (E_{P1}) and calculating the energy of D at that same geometry (E_{P2}). The average nuclear re-organisation energy associated with the donor unit can be calculated from the following equation:

$$\lambda_1 = E_{P1} - E_{R1}$$
$$\lambda_2 = E_{P2} - E_{R2} \quad (25)$$
$$\lambda = \lambda_1 + \lambda_2$$

The same procedure holds for the acceptor part of the molecule.

4. Solvent re-organisation energy

4.1. FDPB

The solvent re-organisation energy (λ_0) associated with electron-transfer in a D–B–A system can be estimated qualitatively using the following equation [10]:

$$\lambda_0 = e^2 \left(\frac{1}{2r_D} + \frac{1}{r_A} - \frac{1}{r}\right)\left(\frac{1}{n^2} - \frac{1}{\varepsilon_s}\right) \quad (26)$$

Here, r_D and r_A are the radii of D and A, respectively, r is the D–A centre-to-centre separation distance, while n and ε_s are the refractive index and dielectric constant of the solvent, respectively. The problem with applying this expression lies with the uncertainty about the dimensions of the various species, especially the separation distance. As a viable alternative, we note that the electrostatic continuum model [49] has been used successfully to quantify the solvation energy and the reduction potentials for ionised molecules in a polar solvent. The finite difference method is used to solve the appropriate Poisson-Boltzmann equation:

$$\nabla\varepsilon(r)\nabla\varphi(r) + 4\pi\rho(r) = 0 \quad (27)$$

where ε, φ, and ρ are the dielectric constant of the medium, the electrostatic potential, and the charge density, respectively. The electrostatic potential from this equation can be used to calculate the solvent re-organisation energy for the system under investigation as follows:

$$\lambda_0 = \frac{1}{2}\sum_i \Delta q_i(\varphi_i^{\varepsilon_0} - \varphi_i^{\varepsilon_\infty}) \quad (28)$$

Here, Δq_i is the change in partial atomic charge caused by electron-transfer from D to A, and ε_0 and ε_∞ are the static and optical dielectric constants of the solvent, respectively. Note that the term "solvent" could equally well apply to a protein matrix. This method has been exploited by Beratan and co-workers [47,48] and other research groups [49–60] to compute values for the solvent re-organisation energy and for the overall reaction free-energy change associated with electron-transfer. This latter situation is especially interesting because it provides an independent method for calculating the thermodynamic driving force for electron-transfer. Typical results calculated for the structures shown in Fig. 5 are compiled in Fig. 6 [39].

4.2. Marcus two-sphere model

The solvent re-organisation energy at any temperature can be calculated from a standard temperature according to the following equation [48]:

$$\lambda_0(T) = \lambda_0(295) + \Delta\lambda_0(T) \quad (29)$$

In the Marcus two-sphere model, the magnitude of $\Delta\lambda_0(T)$ is computed using the following equation [8,9]:

$$\Delta\lambda_0(T) = \frac{e^2}{2}\left(\frac{1}{r_A} + \frac{1}{r_D} - \frac{2}{R_{CC}}\right) \times \left[\left(\frac{1}{n(T)^2} - \frac{1}{\varepsilon(T)}\right) - \left(\frac{1}{n(295)^2} - \frac{1}{\varepsilon(T)}\right)\right] \quad (30)$$

where n is the refractive index of the solvent having a dielectric constant of ε. More details and specific applications can be found elsewhere [53,58–60].

5. Change in Gibbs reaction free-energy

5.1. Spherical ions model

According to Rehm and Weller [61], the change in reaction free-energy of light-induced electron-transfer in a D–B–A system can be approximated using the following equation:

$$\Delta G^\circ = -E_{00} + E_{OX} - E_{RED} + C \quad (31)$$

Here, E_{00} is the zero–zero optical transition energy, while E_{OX} and E_{RED} are the oxidation and the reduction potentials of the donor and acceptor, respectively. The term C is a constant that accounts for electrostatic and solvation terms and which can be estimated on the basis that both donor and the acceptor species are spherical with radii r_D and r_A, respectively:

$$C = \frac{e^2}{2}\left(\frac{1}{r_A} + \frac{1}{r_D} - \frac{2}{R_{CC}}\right)\left(\frac{1}{\varepsilon(T)} - \frac{1}{\varepsilon_{REF}}\right) - \frac{e^2}{\varepsilon_{REF}R_{CC}} \quad (32)$$

Here, R_{CC} is the centre-to-centre distance between the donor and acceptor, $\varepsilon(T)$ is the temperature-dependent dielectric constant of the surrounding solvent, and ε_{REF} is the reference dielectric constant in which the redox potentials were measured. The method has obvious limitations, especially when D and A are far from the spherical. Furthermore, the temperature dependence of the solvent dielectric constant contributes towards the temperature dependence of the change in reaction free-energy. The results for selected target molecules are given in Fig. 7 [48].

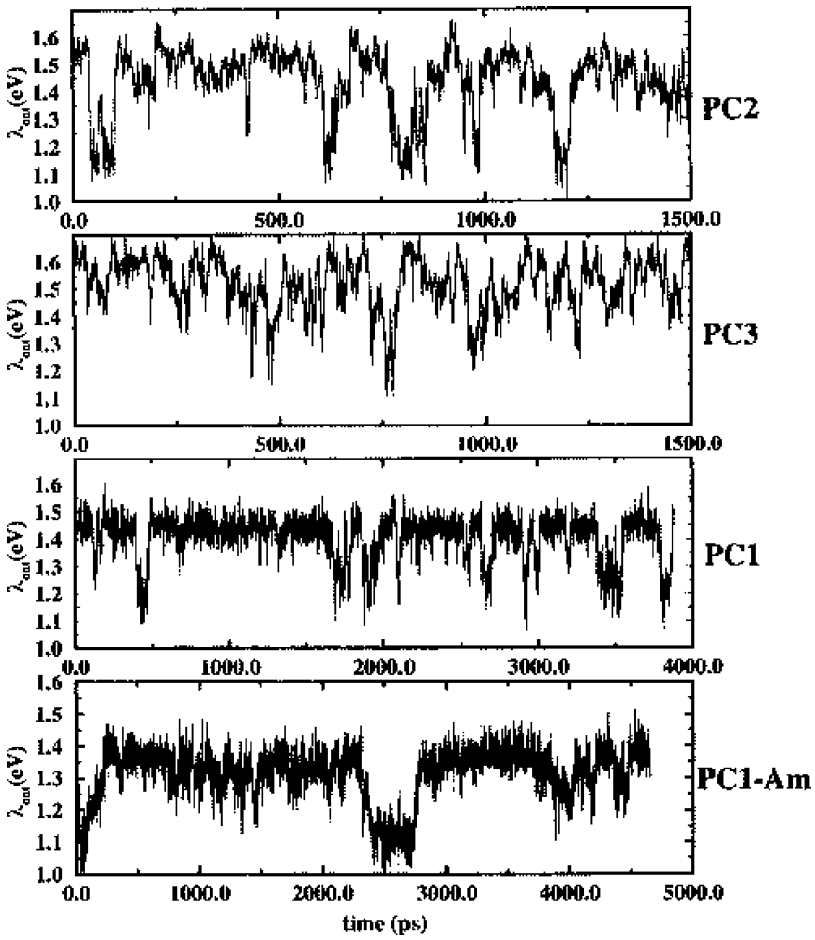

Fig. 6. Time-dependence for the solvent re-organisation energies of some of the molecules illustrated in Fig. 5, as computed by the FDPB and molecular dynamics methods (see [47] for details).

5.2. FDPB

The change in reaction free-energy for a light-induced electron-transfer reaction can be calculated from the FDPB method by following the sequence outlined below [48]:

1. The D–B–A system is broken into molecular fragments corresponding to DB and BA.
2. The redox potentials of DB and BA are found in an appropriate polar solvent:

$$DB_s + BA_s \rightarrow D^+B_s + BA_s^- \quad (E_{OX} - E_{RED})$$

3. The ions are transferred to a medium possessing the same dielectric constant as that of the bridge:

$$D^+B_s + BA_s^- \rightarrow D^+B_B + BA_B^- \quad (-\Delta G_{solv}^{D^+B} - \Delta G_{solv}^{BA^-})$$

4. Transfer the charges of both species to the D–B–A:

$$DBA_B + D^+B_B + BA_B^- \rightarrow D^+BA_B^- + DB_B + BA_B \quad (\Delta G_B^{Coul})$$

5. Transfer the charge transfer state (CTS) to the polar solvent:

$$D^+BA_B^- \rightarrow D^+BA_s^- \quad (\Delta G_{solv}^{CTS})$$

6. Transfer the neutral fragments to the same polar solvent:

$$DB_B + BA_B \rightarrow DB_s + BA_s \quad (\Delta G_{trans})$$

7. Transfer the neutral species D–B–A from the polar solvent to the medium with the same dielectric constant as the bridge:

$$DBA_s \rightarrow DBA_B \quad (-\Delta G_{trans}^{GS})$$

8. Calculate the excitation energy for the electronic state prior to electron-transfer (this state is usually a locally-excited singlet state (LESS):

$$D^*BA_s \rightarrow DBA_B \quad (-E_{00})$$

9. Add all of the above steps together in order to find the reaction free-energy:

$$D^*BA_s \rightarrow D^+BA_B^-$$

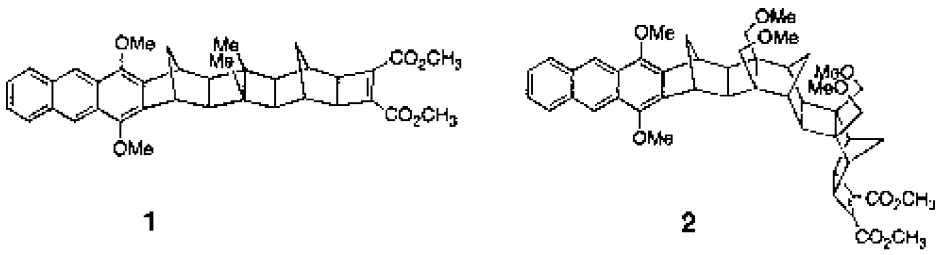

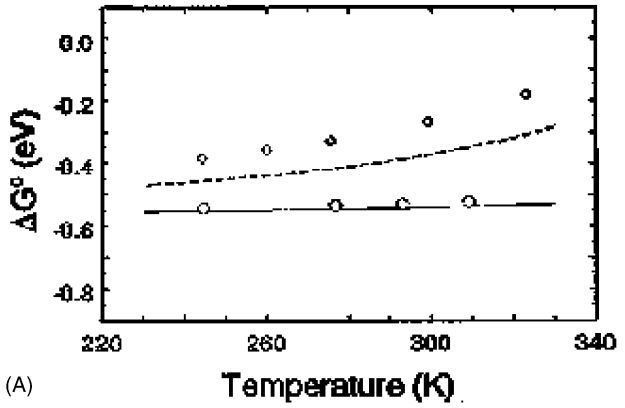

(A)

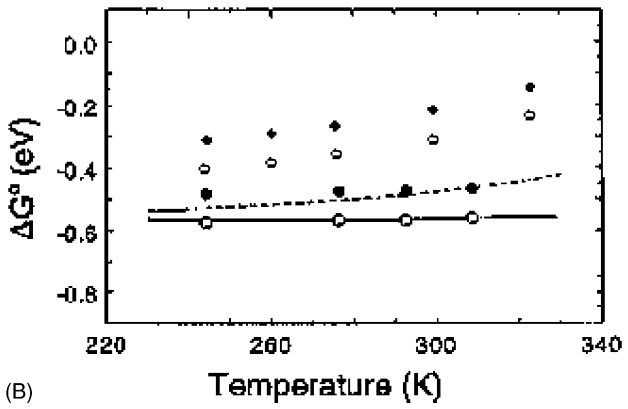

(B)

Fig. 7. The molecular structures used for calculations and the derived values for $\Delta G^{\circ}(T)$ as computed by the two-sphere model and by the FDPB method. (A) Compound **1** in THF (◇) and acetonitrile (○). (B) Compound **2** in THF (◇ and ◆) and acetonitrile (○ and ●) (see [48] for details).

$$\Delta G^{\circ} = -E_{00} - \Delta G^{\mathrm{GS}}_{\mathrm{trans}} + \Delta G_{\mathrm{trans}} + \Delta G^{\mathrm{CTS}}_{\mathrm{solv}} + \Delta G^{\mathrm{Coul}}_{\mathrm{B}} - \Delta G^{\mathrm{D^+B}}_{\mathrm{solv}} - \Delta G^{\mathrm{BA^-}}_{\mathrm{solv}} + E_{\mathrm{OX}} - E_{\mathrm{RED}}$$

This method is illustrated in Fig. 7 by way of a typical calculation [48].

6. Coupling element

6.1. Transition density cubes (TDC) method

Consider a system in which the donor is first promoted to its first-allowed excited state by transfer of an electron from an occupied MO d to an unoccupied MO d′. By energy transfer from donor to acceptor, we could have a transition from MO a to a′ of the acceptor. If we ignore any direct overlap between the MOs of D and A, the only coupling between two moieties would be due to Coulombic interactions:

$$V^{\mathrm{Coul}} = 2(\mathrm{d}'\mathrm{d}|\mathrm{aa}') = 2\int \mathrm{d}'(1)\mathrm{a}(2) r_{12}^{-1} \mathrm{d}(1)\mathrm{a}'(2)\,\mathrm{d}\tau \quad (33)$$

The extent of Coulombic coupling between donor and acceptor units can be expressed in terms of the transition density [62]:

$$V^{\mathrm{Coul}} = \sum_{ij} \frac{M^{\mathrm{eq}}_{\mathrm{D}}(i) M^{\mathrm{eq}}_{\mathrm{A}}(j)}{4\pi\varepsilon_0 r_{ij}} \quad (34)$$

Here, M_N refers to the transition density for molecule N:

$$M^{\mathrm{eq}}_N = \int_s \psi_{N\mathrm{g}} \psi^*_{N\mathrm{e}}\,\mathrm{d}s\,\mathrm{d}r \quad (35)$$

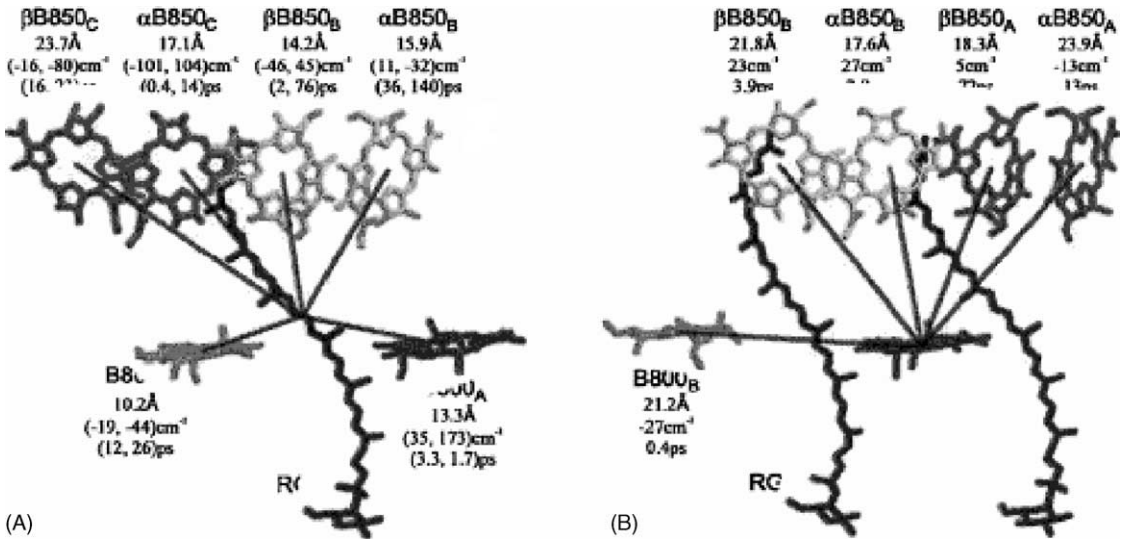

Fig. 8. (A and B) Coupling strengths and the energy transfer time constants for transitions between the various chromophores in the bacterial light-harvesting complex (see [66] for details).

The integral is taken over the spin density and ψ_{Ng} and ψ_{Ne} are the wave functions of the molecule N in its' ground and excited states, respectively. The TDC are obtained from subsequent quantum mechanics calculation and a configuration interaction (CI) calculation has to be performed for the wave functions associated with the excited states. This method has been used successfully for computing the extent of electronic coupling between the pigments involved in photosynthetic reaction centres as well as the mechanism of energy transfer between pigments in the corresponding light-harvesting complex [63–72]. A summary of the results of one such calculation is provided by way of Fig. 8 [66].

Application of the above-mentioned method requires access to the transition density matrix. This parameter can be found conveniently using post Hartree–Fock quantum chemical approaches [72,73]. It is necessary first to identify the nature of the relevant excited state by performing a CI calculation which gives the relative contributions of the configurations involved in the electronic transition (C_j). This calculation also exposes the coefficients of the atomic orbitals for those MOs relevant to the transition (c_q^{occ} and c_q^{unocc} for the coefficients of the atomic orbital q in the occupied and unoccupied MOs, respectively). The transition density between atomic orbital q and r is found from the following equation:

$$\rho(q,r) = \frac{1}{\sqrt{2}}\left[\sum_j C_j c_q^{\text{occ}} c_r^{\text{unocc}} + \sum_j C_j c_q^{\text{unocc}} c_r^{\text{occ}}\right] \quad (36)$$

where ρ is the density matrix and has the following property:

$$\sum_q \sum_r |\rho(q,r)|^2 = 1 \quad (37)$$

Fig. 9 shows the results of the transition density calculation for the Q_x and Q_y transitions belonging to the ground state in bacteriochlorophyll [63], this molecule being a principal component of the light-harvesting complexes in purple bacteria.

6.2. Perturbation theory

In D–B–A systems, it is assumed that the atomic orbitals of the donor and acceptor are linked to the adjacent atomic orbitals of the bridge. The electronic coupling matrix element for this system can be calculated from perturbation theory as follows:

$$H_{\text{DA}} = \sum_{\text{v}} \frac{\gamma_{\text{v}}\delta_{\text{v}}}{\varepsilon_{\text{v}} - \varepsilon_{\text{t}}} \quad (38)$$

Here, ε_{v} and ε_{t} refer to the energy of MO 'v' and the tunnelling energy (i.e. the energy of the localised MO on D), respectively, and

$$\gamma_{\text{v}} = \sum_j \sum_l c_l^{\text{D}} \lambda_{lj} c_{j\text{v}}$$
$$\delta_{\text{v}} = \sum_k \sum_m c_m^{\text{A}} \lambda_{km} c_{k\text{v}} \quad (39)$$

where j and k denote the atomic orbitals of the bridge and l and m refer to the atomic orbitals localised on D and A, respectively. The terms λ_{lj} and λ_{lj} account for any interaction between the atomic orbitals of the donor or acceptor and the atomic orbitals of the bridge. These latter terms can be calculated using the Wolfsberg–Helmholtz approximation [74]:

$$\lambda_{lj} = \tfrac{1}{2} K S_{lj} (\varepsilon_l + \varepsilon_j) \quad (40)$$

where K is a constant that is usually considered to have a numerical value of 1.75, S_{lj} describes the extent of overlap between l and j, whilst ε_l and ε_j, respectively, refer to the energy of the atomic orbitals specific to D and the bridge.

Siddarth and Marcus [75] studied a range of organic and organometallic compounds using the above equations,

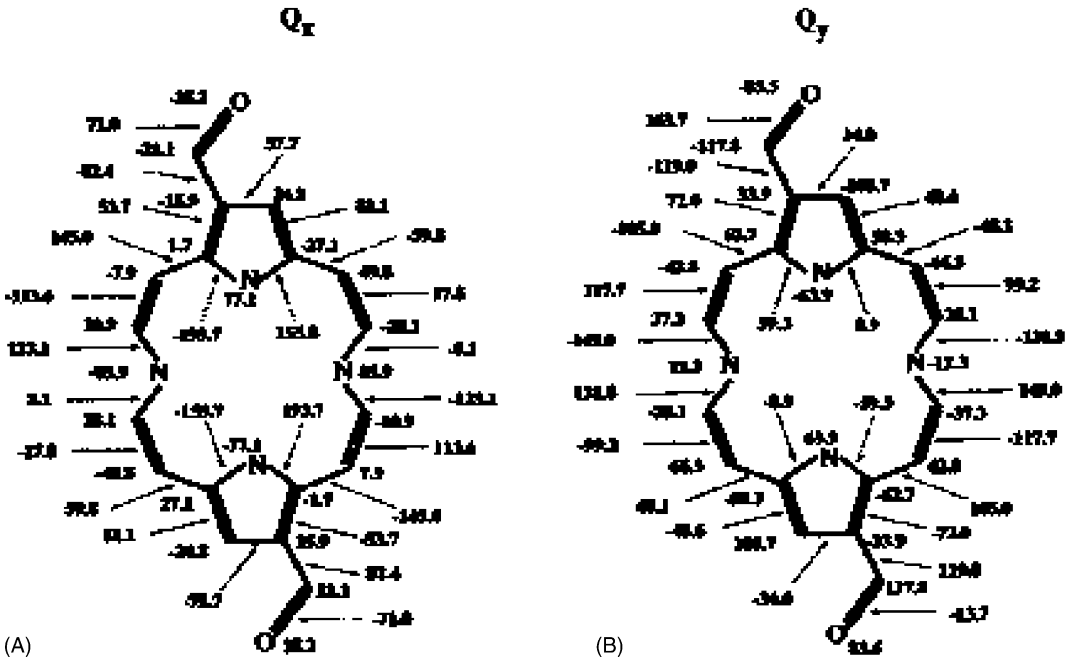

Fig. 9. Transition density matrix elements for (A) the Q_x to ground state transition and (B) the Q_y to ground-state transition (see [63] for details).

as well as the two-state model described in the current manuscript. They compared their computational results to the available experimental data and showed that the perturbation method can give a meaningful description of electron-transfer in such molecules [75]. Fig. 10 illustrates the structures and the main results from this work. Closely-related calculations have now been done on various systems [76–79] and it is clear that this approach can be highly effective.

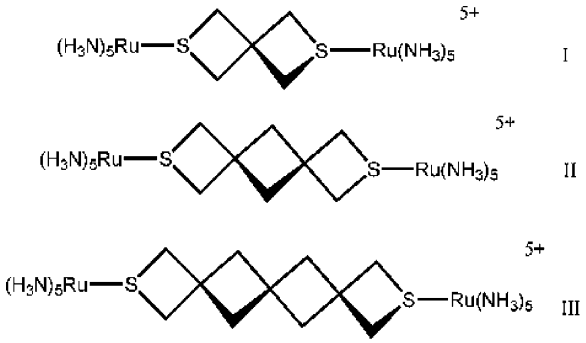

Compound	Calculated H_{DA} / cm^{-1}	Experimental[a] / cm^{-1}
I	171	138
II	57	55
III	20	24

a. C. A. Stein, H. J. Taube, J. Am. Chem. Soc., 1981, *103*, 693.

Fig. 10. Structures and electronic coupling matrix elements calculated for structures based on $Ru(NH_3)_5^{2+}$–$Ru(NH_3)_5^{3+}$ with different dithiaspiro-based bridges (see [75] for details).

6.3. Distance dependence of the coupling element

One of the most important issues in electron-transfer concerns understanding how the electronic coupling matrix element varies with the distance separating the donor from the acceptor. If we restrict attention to rigid molecules of generic description D–B–A, and as the first approximation neglect nuclear motions, it is relatively straightforward to compute the distance dependence. This can be done simply by injecting an electron into the system. The extra electron should go to the first virtual orbital of the molecule. In most D–B–A systems, orbitals localised on the bridge lie outside the energy range of the donor and acceptor units. As such, this extra electron is most likely associated with a LUMO resident on either donor or acceptor. In order to follow electron-transfer, we have to identify the appropriate wave functions belonging to the donor and acceptor. The required virtual orbitals can be specified as being associated with the donor, φ_1, and the acceptor, φ_2. In the absence of significant mutual interactions, these orbitals will be degenerate. Now, we can mix these orbitals to produce two new wave functions:

$$\psi_+ = \frac{1}{\sqrt{2}}(\varphi_1 + \varphi_2)$$
$$\psi_- = \frac{1}{\sqrt{2}}(\varphi_1 - \varphi_2) \quad (41)$$

The resulting orbitals have different energies. Solving the secular equation for these orbitals gives their energies as follows:

$$E_\pm = \tfrac{1}{2}[(E_1 + E_2) \pm \sqrt{(E_1 - E_2)^2 + 4\,|H_{12}|^2}] \quad (42)$$

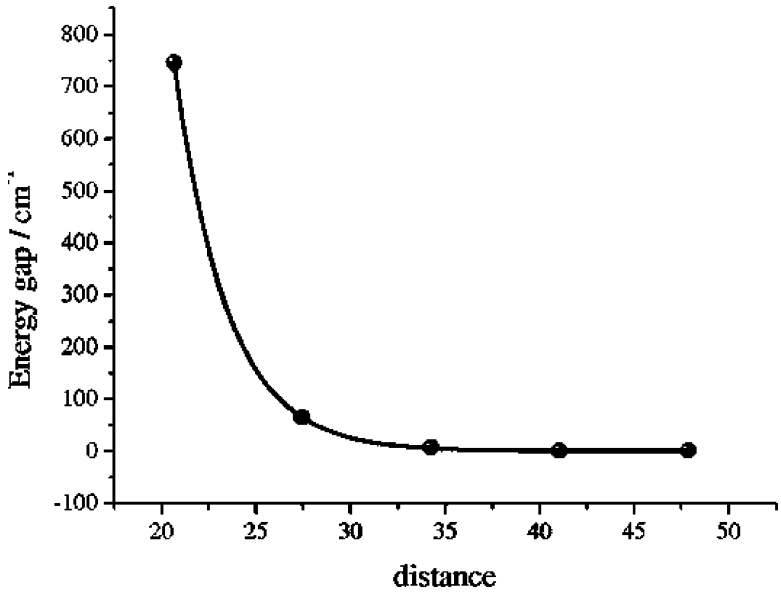

Fig. 11. Exponential dependence of the energy gap on the length of the bridge for molecules of the generic type: $[Zn(bipy)_3$-(1,4-diethynylenebenzene)$_{n=1-5}$-$Zn(bipy)_3]^{4+}$.

The energy gap between these orbitals is a criterion for electronic coupling between the two terminals of the bridge. McConnell used a second-order perturbation theory to compute this energy gap [80]:

$$\Delta E = E_+ - E_- = -\left(\frac{2T^2}{D}\right)\left(-\frac{t}{D}\right)^{N-1} \quad (43)$$

Here, N is the number of repeat units in the bridge, T is the interaction energy between donor (or acceptor) with the atomic orbitals of the first unit (last unit) in the bridge, t is the interaction energy between adjacent bridge units, and D is the energy difference between the tunnelling energy and the MO energy of the bridge. If we place the added electron in the first orbital at $t = 0$, the electron will be in the last one at $t = h/|\Delta E|$.

Instantaneous injection of an electron into the system creates a set of different configurations. The energies of the two configurations that retain the unpaired electron on either the donor or the acceptor can be found from a CI calculation. The energy difference between these two configurations is defined as the energy gap. It is this energy gap that is inversely related to the electronic coupling matrix element. This energy gap is readily calculated. The length of the bridge can then be varied systematically by adding incremental numbers of repeat units. The calculation is repeated for each bridge so that the relationship between energy gap and separation distance becomes apparent. As an example of this basic methodology, we note that the energy gap between two terminal metal bipyridine complexes bridged by incremental numbers of ethynylated phenylene rings decays exponentially with increasing number of repeat units,[1] as shown in Fig. 11.

[1] Unpublished work.

The effect of separation distance between the donor and acceptor units has been investigated extensively both experimentally and theoretically [81,82]. In a D–B–A system where electronic coupling between the terminals is relatively weak, electron tunnelling usually takes place through the super-exchange mechanism. Under such conditions, the rate of electron-transfer (k) displays an exponential decrease with increasing separation distance (R) between the redox-active subunits:

$$k \propto e^{-\beta R} \quad (44)$$

Here, the distance is measured in units of Å and β is an attenuation factor that has values ranging from about 0.2 $Å^{-1}$ [83–86] to about 1.4 $Å^{-1}$ [87,88]. In order to evaluate β by quantum chemical approaches, appropriate structures of the molecule in the initial and final electronic states (i.e. D–B–A in the reactant state and D^+–B–A^- in the product state) are necessary. For example, the molecular structures shown in Fig. 12 have been studied by Pourtois et al. [89] In this work, all of the parameters relevant to electron-transfer have been calculated and used to explain the experimental observation of how the rate of through-bond (TB) electron-transfer depends on the length of the bridge. Specifically, λ, ΔG°, H_{DA}, the transition dipole moments and the identity of relevant MOs were computed. Fig. 13 shows how the length of the bridge affects the energy gap, the electronic coupling matrix element, and the transition dipole moment. Related work has been carried out on various organic systems [60] as well as for long-range electron tunnelling in DNA [90–95].

6.4. Generalized Mulliken–Hush (GMH) method

According to the generalised Mulliken–Hush treatment [96–100], the electronic coupling matrix element can be

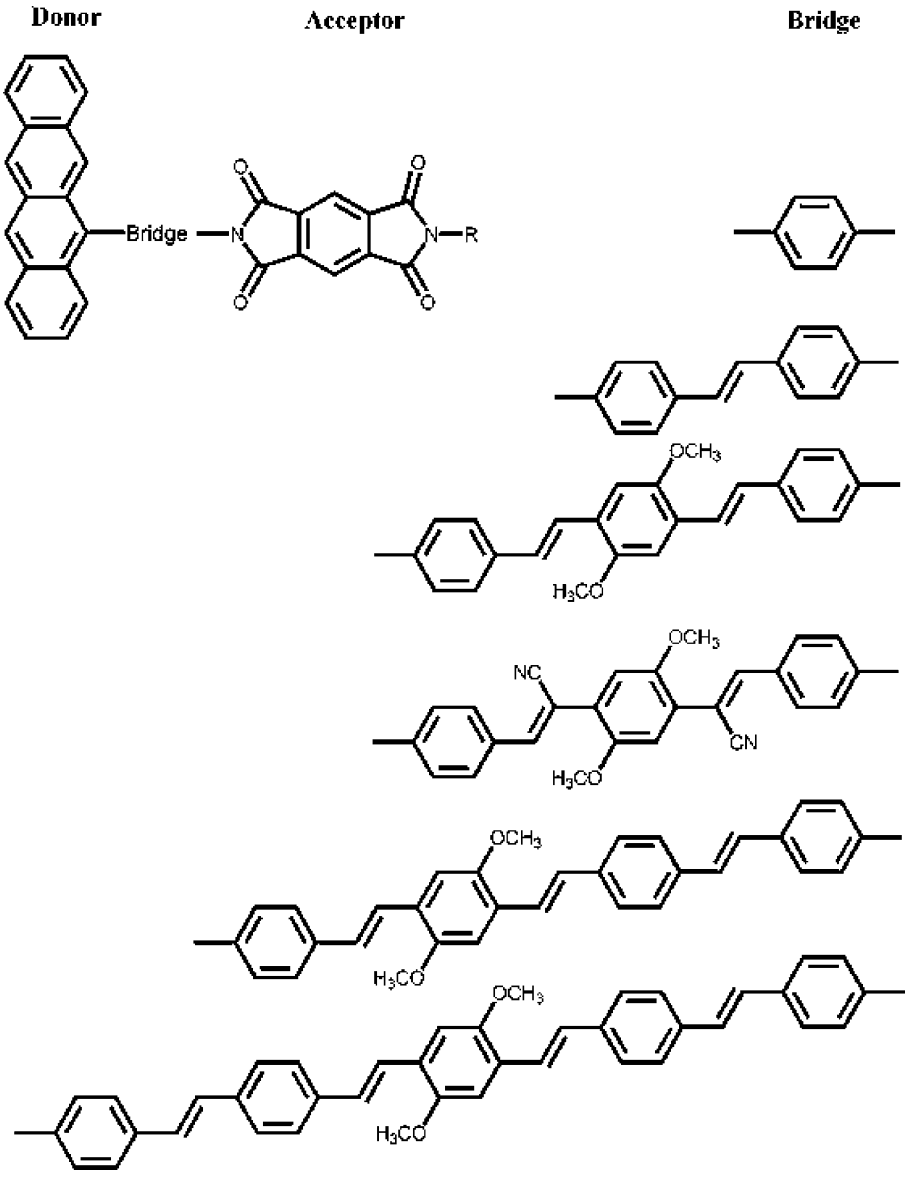

Fig. 12. The molecular structures of the donor, acceptor, and different bridges used by Pourtois et al. (see [89] for details).

evaluated from the following equation:

$$H_{DA} = \frac{\mu_{12}\Delta E_{12}}{\Delta\mu_{ab}} = \frac{\mu_{12}\Delta E_{12}}{\sqrt{[(\Delta\mu_{12})^2 + 4(\mu_{12})^2]}} \quad (45)$$

Here, H_{DA} is the electronic coupling matrix element, μ_{12} is the transition dipole moment between electronic states 1 and 2, ΔE_{12} is the energy gap between the states 1 and 2, and $\Delta\mu_{12}$ is the difference in dipole moment between the two electronic states. To a rough approximation, the difference in dipole moment between the adiabatic states can be approximated as eR_{DA} where R_{DA} is the centre-to-centre separation distance between the donor and acceptor. This method has been developed by Cave and Newton [101] and has become extremely popular because of its simplicity and accuracy [102]. Particular examples of calculating the coupling element by this method can be found in the work of Rust et al. [103] and Elliott et al. [104] Coupling elements of 0.19 and 0.15 eV have been found for electronic coupling between the ground state and the corresponding CTS and between a LESS and the charge-transfer state (CTS), respectively, for the molecule shown in Fig. 14 [102].

6.5. Ab initio molecular orbital calculations of through-space and through-bond electronic coupling matrix elements

It should be recalled that the electronic coupling matrix element associated with intramolecular charge-transfer systems is a combination of through-space (TS) and TB electronic interactions. The extent of TS coupling can be found using the following equation:

$$H_{DA}(TS) = \langle\phi_R|H_{el}|\phi_P\rangle \quad (46)$$

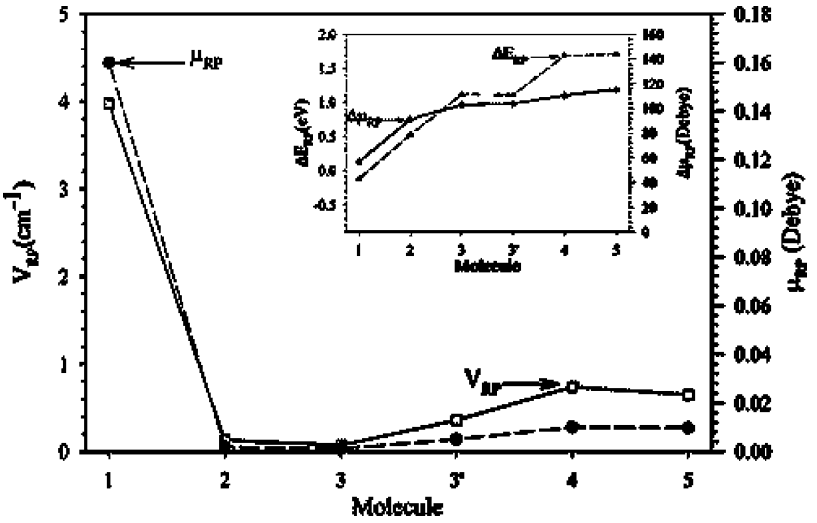

Fig. 13. Electronic coupling matrix elements (V_{RP}), transition dipole moments (μ_{RP}), energy gap (ΔE_{RP}) and the state dipole moment difference ($\Delta\mu_{RP}$) for the D^*BA/D^+BA^- charge-transfer process for the molecules displayed in Fig. 12 (see [89] for details).

Here, H_{el} refers to the electronic Hamiltonian for the system, and ϕ_R and ϕ_P are the electronic wave functions of the reactants and products, respectively. In contrast, the extent of TB coupling can be found using the following relationship:

$$H_{DA}(TB) = \sum_{i,j} H_{RB_i} G_{ij} H_{B_iP} \quad (47)$$

Here, H_{RB} and H_{BP}, respectively, are the Hamiltonian matrix elements of the intermediate states formed by interaction of the bridge with the reactant state and the bridge with the product state. The term G_{ij} is the Green's function corresponding to mutual interaction between adjacent states i and j localised on the bridge states and is calculated using the following equation:

$$G_{ij}(E) = \frac{\delta_{ij}}{E - E_i} + \frac{1}{E - E_i} T_{ij} \frac{1}{E - E_j} + \sum_k \frac{1}{E - E_i} T_{ik} \frac{1}{E - E_k} T_{kj} \frac{1}{E - E_j} + \cdots \quad (48)$$

Here, E refers to the tunnelling energy and E_i is the energy of state i, while T_{ij} is a measure of the coupling between adjacent states of the bridge.

The wave functions of the reactants and of the products are produced by electronic transitions between the MOs of the donor and the acceptor, respectively.

$$|\phi_R\rangle = \sum_{ij} C_{ij} \left|\Psi[\mathrm{OccMO}_{i\mathrm{D}} \rightarrow \mathrm{UnoccMO}_{j\mathrm{D}}\right\rangle \quad (49)$$

$$|\phi_P\rangle = \sum_{kl} C_{kl} \left|\Psi[\mathrm{OccMO}_{k\mathrm{A}} \rightarrow \mathrm{UnoccMO}_{l\mathrm{A}}\right\rangle \quad (50)$$

Here, C_{ij} is the CI coefficient, $\mathrm{OccMO}_{i\mathrm{D}}$ and $\mathrm{UnoccMO}_{j\mathrm{D}}$ refer to the ith occupied MO and the jth unoccupied MO of the donor, respectively. The same wave functions are expected for population of intermediate states localised on the bridge part of the molecule.

The starting point for the calculation involves identifying those MOs associated with the three key components of the supermolecule, namely the donor, bridge and acceptor. The next step is to construct the electronic configurations that are used to compute the energies of the electronic states of the reactants, products, and the bridge. This is done by considering the transitions between the occupied and unoccupied MOs attributable to each part of the molecule. Hayashi and Kato used this method to compute the electronic coupling matrix element for photo-induced electron-transfer from a porphyrin to a quinone through different bridges [105].

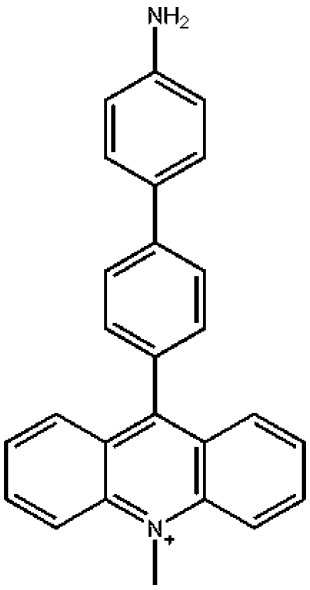

Fig. 14. The molecular structure of 9-(aminophenyl)-10-methylacridinium.

6.6. Avoided-crossing method

Most organic molecules are promoted to the first-excited singlet state under illumination with UV or visible light. This state is often referred to as the LESS and represents the system prior to electron-transfer. After electron-transfer, the system changes its electronic state to a CTS for which there is a substantial increase in dipole moment. This change of state occurs at a point on the PESs drawn for each of the two states. The intersection point is where the energies of the two states are identical. However, the two potential energy curves are not allowed to cross each other at this point because of the avoided crossing rule. The intersection point, therefore, corresponds to the minimum energy gap between the two states. Numerically, this minimum energy gap is described as twice the electronic coupling matrix element [104]. There have been several reports in the literature whereby the avoided-crossing method [6,106–108], or two-state model [5,109], has been used to calculate the electronic coupling matrix element [110,111]. A common feature of all this work is that an external field is used to simulate the effect of fluctuation of the solvent polarisation that brings the two electronic states to resonance. For example, in Fig. 15, a fluoride anion is used to achieve resonance between the two relevant states. The energies of the CTS and of the first-singlet excited state are perturbed by varying the distance between the fluoride ion and one end of the molecule [106]. The main principle behind this approach is that the energy of the LESS is hardly affected by the presence of the anion whereas that of the CTS is strongly disturbed by the approaching anion. Systematic variation of the distance between solute and anion, which can be controlled very precisely, facilitates determination of the minimum energy gap.

6.7. The hopping model for hole transfer in DNA

One of the most topical research areas of recent times relates to understanding the mechanism of oxidative damage and subsequent repair in DNA. Such processes are related to charge transfer along, or through, the DNA duplex [112,113]. It is recognised that of the four base pairs guanine (G) is the most easily oxidised and this residue is where most oxidative damage gets concentrated. In order to explain the statistical distribution for oxidative damage it has been proposed that long-range charge transfer in DNA occurs by a series of short-range hopping steps between the G bases [85,86,114,115]. The process starts by oxidation of an individual guanine to G^+, thereby creating a positive hole on the duplex. The hole moves through the DNA strand by hopping between the G bases until it reaches a GGG residue. The ionisation potential for multiple guanine residues is significantly lower than that for an isolated guanine and so the GGG site functions as a hole trap [116–118]. The process of hole transfer between guanines is reversible, but trapping by the GGG units is irreversible. Several models have been proposed to account for this long-range charge

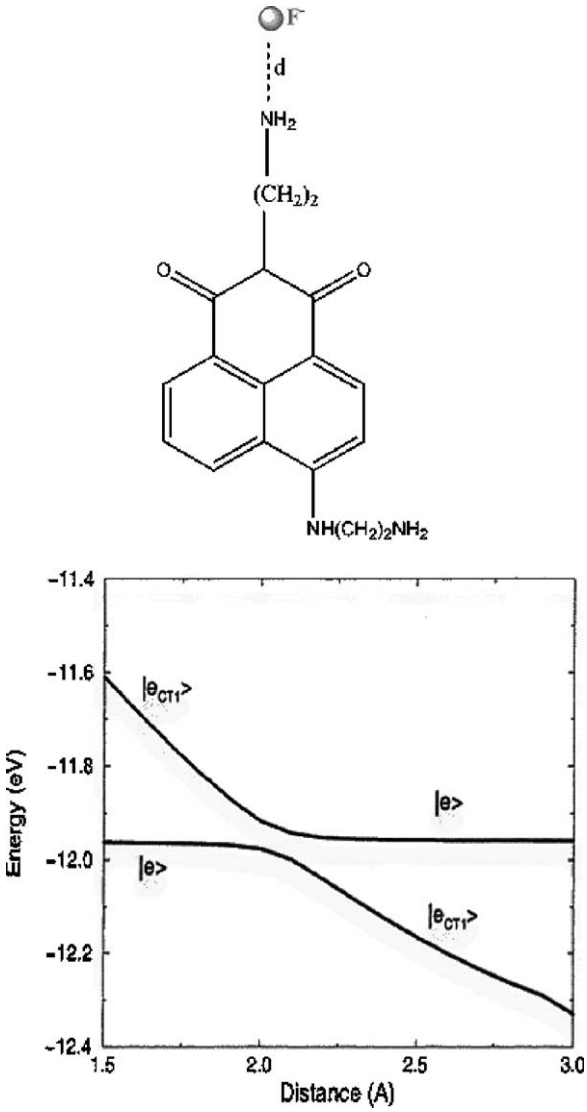

Fig. 15. Top panel: structure of 4-aminonaphthalimide. Bottom panel: the calculated adiabatic curves between the first-excited singlet state (e) and the first charge-transfer state (e_{CT1}) (see [106] for details).

transfer, including a single-step super-exchange mechanism [93] and a multi-step hopping process. In the former case, the rate of charge transport should decrease exponentially with increasing distance travelled by the hole:

$$k = k_0 \exp(-\beta R) \tag{51}$$

In this expression, k_0 is the pre-exponential factor and β is the attenuation factor that describes the ability of the duplex to conduct positive holes.

It has to be realised, however, that both transfer mechanisms can operate together; that is to say, super-exchange theory holds for the tunnelling between the G sites while multi-step hopping accounts for the long-range hole transfer. Direct super-exchange between the initial hole and the GGG acceptor is less effective because of fast exponential decay of the transfer rate. Hole transfer though the guanine bases to the GGG unit is shown schematically in Fig. 16.

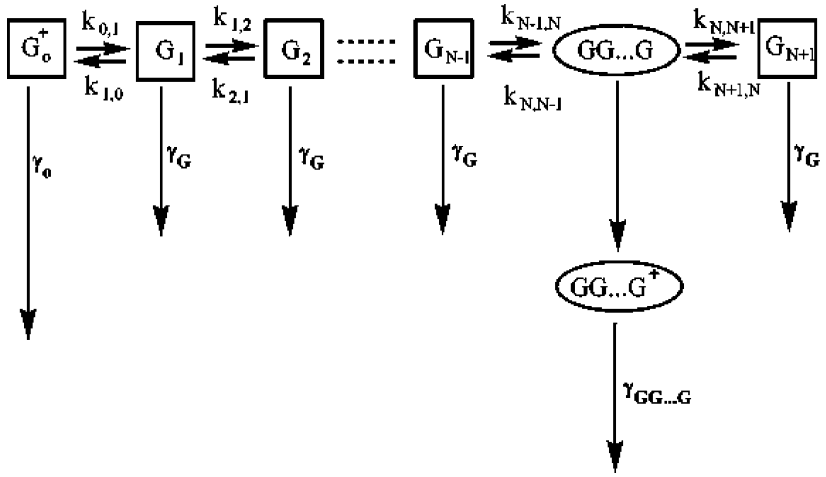

Fig. 16. Schematic representation of the competing rate processes describing hole transfer between guanine sites in DNA (see [94] for details).

The overall mechanism for long-range charge transfer in DNA can now be considered in the following manner: a hole is generated at the first guanine site, G_0, in such a way that several competitive routes are available for its deactivation. These competing processes include; (i) reversible hole transfer to the nearest G base occurring with a forward rate constant of $k_{0,1}$ and a reverse rate constant of $k_{1,0}$, (ii) hole transfer to a water molecule with rate constant γ_0, and (iii) loss of a proton by the initial guanine radical cation to form a neutral radical [119]. The same sequence of competitive process is available for each individual guanine unit in the transport pathway until the positive hole arrives at the *N*th point guanine residue. This latter guanine differs from its predecessors by having a GGG residue nearby. Hole transfer to the multiple guanine unit is rapid, irreversible and results in formation of GGG^+ with a rate constant of k_{rel}. This GGG^+ residue ion can oxidise water with a rate constant of γ_{GGG}. The ratio of reaction products formed from G^+ or GGG^+ reaction with water can be used as an indirect measure of the rate of hole transfer in DNA. Thus, expressing the yield of reaction products from G_j^+ and GGG^+ as Y_j and Y_{GGG}, respectively, the efficiency of hole transfer in terms of the damage ratio can be formulated in two ways:

$$\phi = \frac{Y_{GGG}}{\sum_{j=0}^{N-1} Y_j} = \frac{\int_0^\infty k_{N-1,N} P_{N-1}(t)\,dt}{\int_0^\infty \left[\gamma_0 P_0(t) + \gamma_G \sum_{j=1}^{N-1} P_j(t)\right] dt} \quad (52)$$

$$\phi' = \frac{Y_{GGG}}{Y_0} = \frac{\int_0^\infty k_{N-1,N} P_{N-1}(t)\,dt}{\int_0^\infty \gamma_0 P_0(t)\,dt} \quad (53)$$

Here, P_j is the probability of finding the hole at G_j and can be expressed as follows:

$$\begin{aligned}\frac{dP_j(t)}{dt} &= -\gamma_0 P_j(t)\delta_{j,0} - \gamma_G P_j(t)(1-\delta_{j,0}) \\ &\quad -k_{j,j+1}[P_j(t) - P_{j+1}(t)](1-\delta_{j+1,N}) \\ &\quad -k_{j,j-1}[P_j(t) - P_{j-1}(t)](1-\delta_{j,0}) \\ &\quad -k_{j,j+1} P_j(t)\delta_{j,N-1}\end{aligned} \quad (54)$$

Here, $j = 0, 1, \ldots, N-1$, δ function is the Kronecker delta, while $P_0 = 1$ and $P_{j\neq 0} = 0$ at $t = 0$. If $k_{0,1} = k_{1,2} = \cdots = k$, and $\gamma_0 = \gamma_G = \gamma$, then we have

$$\phi = \frac{k}{\gamma} \frac{2\sinh(\sqrt{\gamma/k})\sinh(\sqrt{\gamma/k}/2)}{\cosh((N+1/2)\sqrt{\gamma/k}) - \cosh(\sqrt{\gamma/k}/2)} \quad (55)$$

$$\phi' = \frac{k}{\gamma} \frac{\sinh(\sqrt{\gamma/k})}{\sinh(N\sqrt{\gamma/k})} \quad (56)$$

where N is the number of guanine sites. The values of the various parameters required for the above equations can be found from the experimental data [90–95].

Two types of electronic coupling have to be considered when accounting for hole transfer between the pairs of nucleobases in DNA: namely, intrastrand coupling between bases on a single strand and interstrand coupling between bases of a duplex. In the two-state model, the electronic coupling is estimated as half the energy splitting between the adiabatic states of donor and acceptor [5]. However, the minimum energy splitting can also be calculated by applying an external perturbation, such as an electric field [109]. At this point, the donor and acceptor are in resonance.

In Watson–Crick base pairs (WCP), the HOMO and HOMO-1 are located on the purine nucleobases (namely, guanine and adenine) whereas the HOMO-2 and HOMO-3 are mainly localised on the pyrimidine nucleobases (namely, cytosine and thymidine). Using Koopman's theorem, it is possible to estimate the adiabatic states as the HOMO and the HOMO-1 and the energy splitting as the energy difference between these two MOs. More details can be found elsewhere [110,111].

6.8. The pathways method

The so-called pathway model introduced by Beratan and co-workers [120–125] provides an alternative method for calculating the magnitude of the electronic coupling matrix element, especially in protein matrices. In this approach,

the donor and acceptor are considered to be connected by a protein-based bridge, which mediates electronic coupling between the redox-active partners. Coupling between the donor and acceptor involves a variety of physical tunnelling pathways that can be defined as a collection of interacting bonds, hydrogen bonds, and interactions through space (or van der Waals interactions). Furthermore, we can define a set of parameters ε_C, ε_H, and ε_S that describe the attenuation of electronic coupling through these individual covalent bonds, hydrogen bonds, and TS coupling, respectively. The magnitude of these parameters can be found using the following equations:

$$\begin{aligned}\varepsilon_C &= 0.6\\ \varepsilon_H &= 0.36\exp[-1.7(R-2.8)]\\ \varepsilon_S &= 0.6\exp[-1.7(R-1.4)]\end{aligned} \quad (57)$$

Here, R is the distance between the interacting orbitals, 1.4 and 2.8 are the equilibrium lengths of covalent and hydrogen bonds in Å, respectively, and 1.7 is the attenuation factor. The electronic coupling matrix element is found for each pathway as

$$t_{DA} = (\text{prefactor})\prod_{i=1}^{N_C}\varepsilon_C(i)\prod_{j=1}^{N_S}\varepsilon_S(j)\prod_{k=1}^{N_H}\varepsilon_H(k) \quad (58)$$

Some examples of results collected by this method are found in the above-mentioned references, as well as in the work of Regan et al. [126] and Ullmann and Kostiæ [127].

6.9. Trajectory surface hopping (TSH)

The trajectory surface hopping (TSH) methodology, which was developed recently by Tully and co-workers [128–132], has been applied to the detailed investigation of hole transfer processes in the set of molecules illustrated in Fig. 17 [133]. The method starts out by assuming that the positive hole is localised on the first double bond. As the reaction proceeds, structural distortion within the molecule modulates the bond lengths of the two unsaturated bonds and, at certain times, these bond lengths become identical. Effectively, this results in delocalisation of the hole over the two double bonds. If we represent the wave functions of the hole localised on the left and right double bonds as being ψ_L and ψ_R, respectively, the resulting wave function of the system with equal hole contributions from the two double bonds becomes $2^{-1/2}(\psi_L + \psi_R)$ or $2^{-1/2}(\psi_L - \psi_R)$ because of the avoided crossing rule. At the avoided crossing, the electronic coupling matrix element is equal to half the energy gap between the adiabatic states. CI calculations can be used to compute the energies of the two adiabatic states relevant to hole transfer. In order to effect the geometrical changes needed to locate the avoided crossing area it is necessary to conduct a series of MD simulations.

As illustrated in Fig. 18, where the horizontal lines represent the total energy of different hypothetical trajectories, there are three possibilities for the system during the MD simulations.

Case A: The total energy is insufficient for hole (or electron) transfer.

Case B: The total energy is sufficient to facilitate hole (or electron) transfer, but it is insufficient to access the upper adiabatic state.

Case C: The total energy is sufficient for hole (or electron) transfer and also sufficient for accessing the upper adiabatic state.

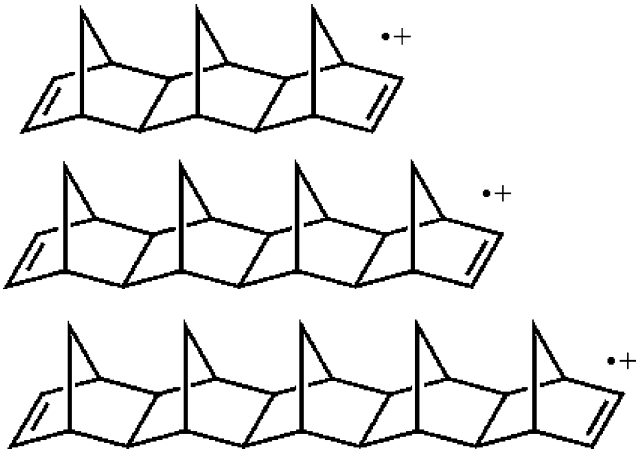

Fig. 17. The polyatomic organic systems used for trajectory surface hopping calculations (see [133] for details).

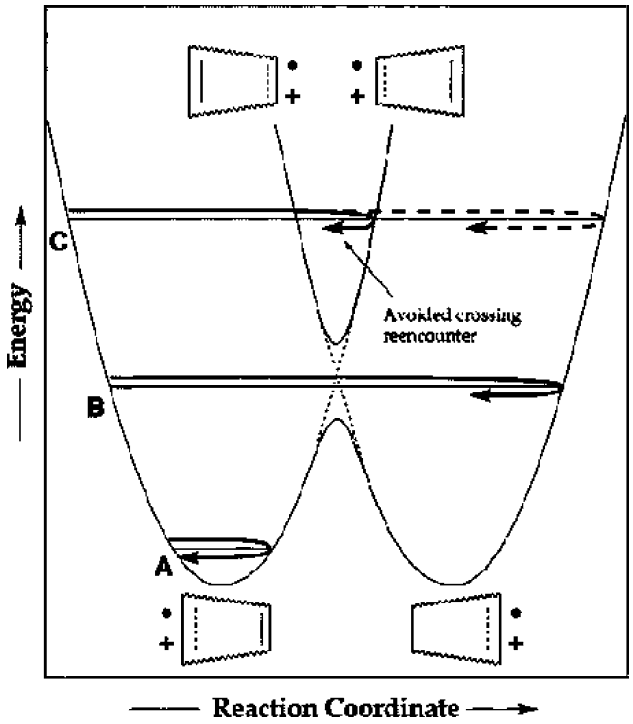

Fig. 18. Behaviour of various trajectories on the adiabatic potential energy surfaces (see [133] for details).

Now, TSH is considered to occur only in case C. The probability of hole (or electron) transfer can be estimated from the Landau–Zerner model [134–137]:

$$P = 1 - e^{-2\pi\gamma} \tag{59}$$

Here,

$$\gamma = \frac{H_{12}^2}{\hbar\upsilon|s_1 - s_2|} \tag{60}$$

and P is the probability of the system remaining on the lower state, H_{12} is the electronic coupling matrix element, υ is velocity of motion along the reaction co-ordinate, and s_1 and s_2 represent the first derivatives of the potential energy with respect to the reaction co-ordinate. It is now easy to show that:

$$\upsilon|s_1 - s_2| = \frac{d|\Delta E_{adiabatic}|}{dt} \tag{61}$$

Shown in Fig. 19 are the results of a TSH calculation made for molecule **1**. The calculation produces meaningful values for the energy gap, the electronic coupling matrix element and the other parameters for this molecule [133]. These calculations also make use of the dynamic reaction co-ordinates (DRC) method, as described later. More details are available elsewhere [138].

6.10. Dynamics reaction co-ordinate (DRC)

The DRC method, as introduced by Stewart et al. [139], is based on conservation of the total energy of the system; this means that when the kinetic energy of the system changes the potential energy must change in the opposite direction. This method is very similar to the MD simulations, but with the noted exception that quantum chemical calculations can be made in addition to the usual bond-forming and bond-breaking processes. This method is time-dependent and results in a profile for the change in potential energy versus time, after a particular molecular vibration. The kinetic energy added to the system appears as the motion of the molecule in a direction that is the natural motion of the molecule. The dynamics reaction co-ordinate approach has been applied for the calculation of a transition state structure that relaxes either to product or reactant states. However, it appears that this highly innovative methodology could have important applications for the calculation of the dynamics of the two discrete electronic states involved in electron-transfer.

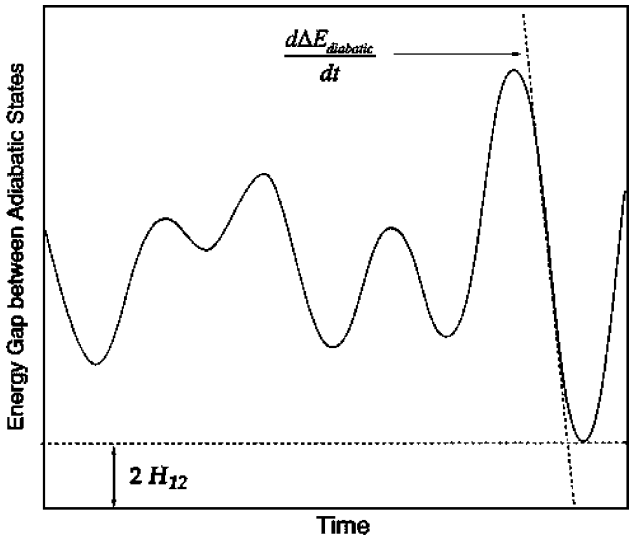

Fig. 19. The calculated Landau–Zener parameters from molecular dynamics simulations and the schematic representation of the derived coupling element (see [133] for details).

7. Conclusion

It is clear that quantum chemistry, with its powerful computational approaches, has an important role to play in electron-transfer. Relatively simple methods are now available for the calculation of nuclear re-organisation energies and electronic coupling matrix elements. These are the two most important parameters for controlling the rate of intramolecular electron-transfer. These terms are highly sensitive to the nature of the reactants and therefore the ability to calculate meaningful values from first principles is a major advance. That there are several different ways to calculate the same parameter is also of great significance. For well-defined systems it is possible to calculate the change in the free-energy of activation for an electron-transfer step. This allows screening of various molecular structures prior to undertaking a lengthy synthetic programme.

All the computational methods mentioned in this article have been tested extensively and found to be valid for examining light-induced electron-transfer. Dealing with excited state reactions adds several extra levels of complexity but nonetheless viable rates of photo-induced electron-transfer can now be calculated. The involvement of transition metals is still a problem but can be handled with certain density functional theory methods. The basic methods are also applicable to biological macromolecules and this area has seen some of the most impressive studies. Armed with these various computational chemistry tools it is now possible to examine in detail factors such as orientational control of electronic coupling.

Acknowledgements

We thank the EPSRC and the University of Newcastle for financial support.

References

[1] J.T. Hynes, Outer-sphere electron-transfer reactions and frequency-dependent friction, J. Phys. Chem. 90 (1986) 3701–3706.

[2] K.V. Mikkelsen, M.A. Ratner, Dynamical theory of electron-transfer: inclusion of inner-shell re-organisation, J. Chem. Phys. 90 (1989) 4237–4247.
[3] K.V. Mikkelsen, M.A. Ratner, Dynamical theory of electron-transfer reactions: bridge-assisted transfer, J. Phys. Chem. 93 (1989) 1759–1770.
[4] P.F. Barbara, T.J. Meyer, M.A. Ratner, Contemporary issues in electron-transfer research, J. Phys. Chem. 100 (1996) 13148–13168.
[5] M.D. Newton, Quantum chemical probes of electron-transfer kinetics: the nature of donor-acceptor interactions, Chem. Rev. 91 (1991) 767–792.
[6] R.A. Marcus, N. Sutin, Electron-transfer in chemistry and biology, Biochim. Biophys. Acta 811 (1985) 265–322.
[7] R.A. Marcus, Electron-transfer reactions in chemistry. Theory and experiment, Rev. Mod. Phys. 65 (1993) 599–610.
[8] R.A. Marcus, The theory of oxidation–reduction reactions involving electron-transfer: part I, J. Chem. Phys. 24 (1956) 966–978.
[9] R.A. Marcus, Electrostatic free-energy and other properties of states having non-equilibrium polarization: part I, J. Chem. Phys. 24 (1956) 979–989.
[10] R.A. Marcus, H. Eyring, Chemical and electrochemical electron-transfer theory, Annu. Rev. Phys. Chem. 15 (1964) 155–196.
[11] M.D. Newton, N. Sutin, Electron-transfer reactions in condensed phases, Annu. Rev. Phys. Chem. 35 (1984) 437–480.
[12] A. Warshel, R.M. Weiss, An empirical valence bond approach for comparing reactions in solutions and in enzymes, J. Am. Chem. Soc. 102 (1980) 6218–6226.
[13] A. Warshel, S.T. Russell, An empirical valence bond approach for comparing reactions in solutions and in enzymes, Q. Rev. Biophys. 17 (1984) 283–422.
[14] L. Pauling, The Nature of the Chemical Bond, Cornell University Press, Ithaca, NY, 1960.
[15] C.A. Coulson, U. Danielsson, Ionic and covalent contributions to the hydrogen bond, I. Ark. Fys. 8 (1954) 239–244.
[16] C.A. Coulson, U. Danielsson, Ionic and covalent contributions to the hydrogen bond, II. Ark. Fys. 8 (1954) 245–255.
[17] J. Åqvist, A. Warshel, Calculations of free-energy profiles for the staphylococcal nuclease catalysed reaction, Biochemistry 28 (1989) 4680–4689.
[18] J. Åqvist, A. Warshel, Free-energy relationships in metallo-enzyme catalyzed reactions. Calculations of the effects of metal ion substitution in staphylococcal nuclease, J. Am. Chem. Soc. 112 (1990) 2860–2868.
[19] A.K. Churg, R.M. Weiss, A. Warshel, T. Takano, On the action of cytochrome *c*: correlation of geometry changes upon oxidation with activation energies of electron-transfer, J. Phys. Chem. 87 (1983) 1683–1694.
[20] S. Creighton, J.-K. Hwang, A. Warshel, W.W. Parson, J.R. Norris, Simulating the dynamics of the primary charge separation process in bacterial photosynthesis, Biochemistry 27 (1988) 774–781.
[21] W.W. Parson, A.T. Chu, A. Warshel, Re-organisation energy of the initial electron-transfer step in photosynthetic bacterial reaction centers, Biophys. J. 74 (1998) 182–191.
[22] W.W. Parson, Z.T. Chu, A. Warshel, Oscillations of the energy gap for the initial electron-transfer step in bacterial reaction centers, Photosynth. Res. 55 (1998) 147–152.
[23] A. Warshel, Dynamics of reactions in polar solvents. Semi-classical trajectory studies of electron-transfer and proton-transfer reactions, J. Phys. Chem. 86 (1982) 2218–2224.
[24] A. Warshel, J.-K. Hwang, Quantized semi-classical trajectory approach for evaluation of vibronic transitions in harmonic molecules, J. Chem. Phys. 82 (1985) 1756–1771.
[25] A. Warshel, W.W. Parson, Computer simulations of electron-transfer reactions in solution and in photosynthetic reaction centers, Annu. Rev. Phys. Chem. 42 (1991) 279–309.
[26] I. Muegge, P.X. Qi, A.J. Wand, Z.T. Chu, A. Warshel, The re-organisation energy of cytochrome *c* revisited, J. Phys. Chem. B 101 (1997) 825–836.
[27] F.S. Lee, Z.T. Chu, M.B. Bolger, A. Warshel, Calculations of antibody–antigen interactions: microscopic and semi-microscopic evaluation of the free energies of binding of phosphorylcholine analogs to mcpc603, Protein Eng. 5 (1992) 215–228.
[28] K. Schulten, M. Tesch, Coupling of protein motion to electron-transfer: molecular dynamics and stochastic quantum mechanics study of photosynthetic reaction centers, Chem. Phys. 158 (1991) 421–446.
[29] H. Treutlein, K. Schulten, A.T. Brünger, M. Karplus, J. Seisenhofer, H. Michel, Chromophore–protein interactions and the functions of the photosynthetic reaction center: a molecular dynamics study, Proc. Natl. Acad. Sci. U.S.A. 89 (1992) 75–79.
[30] H. Treutlein, K. Schulten, C. Niedermeier, J. Deisenhofer, H. Michel, D. DeVault, Electrostatic control of electron-transfer in the photosynthetic reaction center of *Rhodopseudomonas viridis*, in: The Photosynthetic Bacterial Reaction Centre: Structure and Dynamics, NATO ASI Series A: Life Sciences, vol. 149, Plenum Press, New York, 1988, pp. 369–377.
[31] K. Ando, Photo-induced intermolecular electron-transfer reaction between *N*,*N*-dimethylaniline and anthracene in acetonitrile solution, a theoretical study, J. Chem. Phys. 101 (1994) 2850.
[32] S. Hayashi, S. Kato, Solvent effect on intramolecular long-range electron-transfer reactions between porphyrin and benzoquinone in acetonitrile solution: molecular dynamics calculations of reaction rate constants, J. Phys. Chem. A 102 (1998) 3333.
[33] R.B. Yelle, T. Ichiye, Solvation free-energy reaction curves for electron-transfer in aqueous solution: theory and simulation, J. Phys. Chem. B 101 (1997) 4127.
[34] R.A. Kuharski, J.S. Bader, D. Chandler, M. Sprik, M.L. Klein, R.W. Impey, Molecular model for aqueous ferrous–ferric electron-transfer, J. Chem. Phys. 89 (1988) 3248.
[35] D.A. Zichi, G. Ciccotti, J.T. Hynes, Molecular dynamics simulation of electron-transfer reactions in solution, J. Phys. Chem. 93 (1989) 6261.
[36] B. Brooks, R. Bruccoleri, B. Olafson, D. States, S. Swaminathan, M. Karplus, CHARMM: a program for macromolecular energy minimization, and molecular dynamics calculations, J. Comput. Chem. 4 (1983) 187–217.
[37] J. Åqvist, C. Medina, J.-E. Samuelsson, A new method for predicting binding affinity in computer-aided drug design, Protein Eng. 7 (1994) 385–391.
[38] A. Klimkans, S. Larsson, Reorganisation energies in benzene, naththalene and anthracene, Chem. Phys. 189 (1994) 25–31.
[39] K.M. Rosso, J.R. Rustad, Ab initio calculation of homogeneous outer-sphere electron-transfer rates: application to $M(OH_2)_6^{3+/2+}$ redox couples, J. Phys. Chem. A 104 (2000) 6718–6725.
[40] X. Amashukeli, J.R. Winkler, H.B. Gray, N.E. Gruhn, D.L. Lichtenberger, Electron-transfer re-organisation energies of isolated organic molecules, J. Phys. Chem. A 106 (2002) 7593–7598.
[41] Y. Bu, Y. Ding, F. He, L. Jiang, X. Song, Non-empirical ab initio studies on inner-sphere re-organisation energies of $M^{2+}(H_2O)_6$/$M^{3+}(H_2O)_6$ redox couples at valence basis level, Int. J. Quant. Chem. 61 (1997) 117–126.
[42] Y. Bu, Y. Wang, F. Xu, C. Deng, Direct evaluation of the electron-transfer integral for self-exchange reactions in solution, J. Mol. Struct. 453 (1996) 43–48.
[43] L. Eberson, R. Gonzalez-Luque, J. Lorentzon, M. Merchan, B.O. Roos, Ab initio calculation of inner-sphere re-organisation energies of inorganic redox couples, J. Am. Chem. Soc. 115 (1993) 2898–2902.
[44] Y. Bu, X. Song, C. Deng, An inner-sphere re-organisation model of hetero-exchange electron-transfer reactions of diatomic reactants, Chem. Phys. Lett. 250 (1996) 455–460.
[45] Y. Bu, X. Song, Potential surface at the re-organised state and inner-sphere re-organisation energy for diatomic molecules in gaseous phase electron-transfer processes from ab initio calculations, J. Phys. Chem. 98 (1994) 5049–5051.

[46] S. Jakobsen, K.V. Mikkelsen, S.U. Pedersen, Calculations of intramolecular re-organisation energies for electron-transfer reactions involving organic systems, J. Phys. Chem. 100 (1996) 7411.
[47] I.V. Kurnikov, L.D. Zusman, M.G. Kurnikova, R.S. Farid, D.N. Beratan, Structural fluctuations, spin, re-organisation energy, and tunnelling energy control of intramolecular electron-transfer: the surprising case of electron-transfer in a d_8–d_8 bimetallic system, J. Am. Chem. Soc. 119 (1997) 5690–5700.
[48] K. Kumar, I.V. Kurnikov, D.N. Beratan, D.H. Waldeck, M.B. Zimmt, Use of modern electron-transfer theories to determine electronic coupling matrix elements in intramolecular systems, J. Phys. Chem. 102 (1998) 5529–5541.
[49] D. Sitkoff, B. Honig, Accurate calculation of hydration free energies using macroscopic solvent models, J. Phys. Chem. 98 (1994) 1978–1988.
[50] J. Tomasi, M. Persico, Molecular interactions in solutions: an overview of methods based on continuous distributions of the solvent, Chem. Rev. 94 (1994) 2027–2094.
[51] R. Kaplan, A.M. Napper, D.H. Waldeck, M.B. Zimmt, The role played by orbital energetics in solvent mediated electronic coupling, J. Phys. Chem. A 106 (2002) 1917–1925.
[52] T. Simonson, G. Archontis, M. Karplus, A Poisson–Boltzmann study of charge insertion in an enzyme active site: the effect of dielectric relaxation, J. Phys. Chem. B 103 (1999) 6142–6156.
[53] Y.P. Liu, M.D. Newton, Solvent re-organisation and donor/acceptor coupling in electron-transfer processes: self-consistent reaction field theory and ab initio applications, J. Phys. Chem. 99 (1995) 12382–12386.
[54] Y. Zeng, M.B. Zimmt, Symmetry effects in photo-induced electron-transfer reactions, J. Am. Chem. Soc. 113 (1991) 5107–5109.
[55] Y. Zeng, M.B. Zimmt, Symmetry effects on electron-transfer reactions: temperature dependence as a diagnostic tool, J. Phys. Chem. 96 (1992) 8395–8403.
[56] D.V. Matyushov, Re-organisation energy of electron-transfer in polar liquids. Dependence on reactant size, temperature and pressure, Chem. Phys. 174 (1993) 199–218.
[57] D.V. Matyushov, A molecular theory of electron-transfer reactions in polar liquids, Mol. Phys. 79 (1993) 795–808.
[58] M.D. Newton, M.V. Basilevsky, I.V. Rostov, A frequency-resolved cavity model (FRCM) for treating equilibrium and non-equilibrium solvation energies, Chem. Phys. 232 (1998) 201–210.
[59] M.V. Basilevsky, I.V. Rostov, M.D. Newton, A frequency-resolved cavity model (FRCM) for treating equilibrium and non-equilibrium solvation energies, Chem. Phys. 232 (1998) 189–199.
[60] W.B. Davis, M.A. Ratner, M.R. Wasielewski, Conformational gating of long-distance electron-transfer through wire-like bridges in donor–bridge–acceptor molecules, J. Am. Chem. Soc. 123 (2001) 7877–7886.
[61] D. Rehm, A. Weller, Bonding and fluorescence spectra of hetero-excimers, Z. Phys. Chem. (Munich) 69 (1970) 183–200.
[62] R. McWeeny, Methods of Molecular Quantum Mechanics, second ed., Academic Press, London, 1992.
[63] A. Damjanoviæ, T. Ritz, K. Schulten, Energy transfer between carotenoids and bacteriochlorophylls in the light-harvesting complex II of purple bacteria, Phys. Rev. E 59 (1999) 3293–3311.
[64] A. Damjanoviæ, T. Ritz, K. Schulten, Excitation energy trapping by the reaction center of Rhodobacter Sphaeroides, Int. J. Quant. Chem. 77 (2000) 139–151.
[65] A. Damjanoviæ, T. Ritz, K. Schulten, Excitation transfer in the peridinin–chlorophyll–protein of amphidinium carterae, Biophys. J. 79 (2000) 1695–1705.
[66] B.P. Krueger, G.D. Scholes, G.R. Fleming, Calculation of coupling and energy-transfer pathways between the pigments of LH2 by the ab initio transition density cube method, J. Phys. Chem. B 102 (1998) 5378–5386.
[67] B.P. Krueger, G.D. Scholes, R. Jimenez, G.R. Fleming, Electronic energy transfer from carotenoid to bacteriochlorophyll in the purple bacterium Rhodopseudomonas, J. Phys. Chem. B 102 (1998) 2284–2292.
[68] G.D. Scholes, I.R. Gould, R.J. Cogdell, G.R. Fleming, Ab initio molecular orbital calculations of electronic coupling in the LH2 bacterial light-harvesting complex of Rps. Acidophila, J. Phys. Chem. B 103 (1999) 2543–2553.
[69] T. Ritz, A. Damjanoviæ, K. Schulten, Excitons and excitation transfer in the photosynthetic unit of purple bacteria, J. Luminesc. 76–77 (1998) 310–321.
[70] T. Ritz, A. Damjanoviæ, T. Ritz, K. Schulten, J.-P. Zhang, Y. Koyama, Efficient light harvesting through carotenoids, Photosynth. Res. 66 (2000) 125–144.
[71] X. Hu, T. Ritz, A. Damjanoviæ, T. Ritz, F. Autenrieth, K. Schulten, Photosynthetic apparatus of purple bacteria, Q. Rev. Biophys. 35 (2002) 1–62.
[72] E. Zojer, P. Buchacher, F. Wudl, J. Cornil, J.P. Calbert, J.L. Bredas, G. Leising, Excited-state localization in organic molecules consisting of conjugated and non-conjugated segments, J. Chem. Phys. 113 (2000) 10002–10012.
[73] H.S. Cho, D.H. Jeong, S. Cho, S. Kim, Y. Matsuzaki, K. Tanaka, A. Tsuda, A. Osuka, Photophysical properties of porphyrin tapes, J. Am. Chem. Soc. 124 (2002) 14642–14654.
[74] M. Wolfsberg, L. Helmholtz, The spectra and electronic structure of the tetrahedral ions MnO_4^-, CrO_4^-, and ClO_4^-, J. Chem. Phys. 20 (1952) 837–843.
[75] P. Siddarth, R.A. Marcus, Comparison of experimental and theoretical electronic coupling matrix elements for long-range electron-transfer, J. Phys. Chem. 94 (1990) 2985–2989.
[76] A.B.P. Krueger, G.D. Scholes, S. Larsson, Electron-transfer in chemical and biological systems. Orbital rules for non-adiabatic transfer, J. Am. Chem. Soc. 103 (1981) 4034–4040.
[77] I.R. Gould, R.H. Young, L.J. Mueller, A.C. Albrecht, S. Farid, Electronic coupling matrix elements in acceptor–donor excited states and the effect of charge-transfer character on their radiative rate constants, J. Am. Chem. Soc. 116 (1994) 3147–3148.
[78] J.N. Gehlen, I. Daizadeh, A.A. Stuchebrukhov, R.A. Marcus, Tunnelling matrix element in Ru-modified blue copper proteins: pruning the protein in search of electron-transfer pathways, Inorg. Chim. Acta 243 (1996) 271–282.
[79] J. Wolfgang, S.M. Risser, S. Priyadarshy, D.N. Beratan, Secondary structure conformations and long-range electronic interactions in oligopeptides, J. Phys. Chem. B 101 (1997) 2986–2991.
[80] H.M. McConnell, Intramolecular charge transfer in aromatic free radicals, J. Chem. Phys. 35 (1961) 508–515.
[81] C.A. Naleway, L.A. Curtiss, J.R. Miller, Super-exchange pathway model for long-distance electronic coupling, J. Phys. Chem. 95 (1991) 8434–8437.
[82] M.D. Newton, in: J. Jortner, M. Bixon (Eds.), Advances in Chemical Physics, vol. 1, Wiley, New York, 1999, pp. 303–375.
[83] L.M. Tollbert, Solitons in a box: the organic chemistry of electrically conducting polyenes, Acc. Chem. Res. 25 (1992) 561–568.
[84] T.S. Arrhenius, M. Blanchard-Desce, M. Dvolaitzky, J.-M. Lehn, Molecular devices: caroviologens as an approach to molecular wires—synthesis and incorporation into vesicle membranes, Proc. Natl. Acad. Sci. U.S.A. 83 (1986) 5355–5359.
[85] S.O. Kelley, J.K. Barton, Electron-transfer between bases in double-helical DNA, Science 283 (1999) 375–381.
[86] S.O. Kelley, L.K. Barton, DNA-mediated electron-transfer from a modified base to ethidium: pi-stacking as a modulator of reactivity, Chem. Biol. 5 (1998) 413–425.
[87] C.C. Moser, J.M. Kseske, K. Warncke, R.S. Farid, P.L. Dutton, Nature of biological electron-transfer, Nature 355 (1992) 796–802.
[88] J.R. Winkler, H.B. Gray, Electron-transfer in ruthenium-modified proteins, Chem. Rev. 92 (1992) 369–379.

[89] G. Pourtois, D. Beljonne, J. Cornil, M.A. Ratner, J.L. Bredas, Photo-induced electron-transfer processes along molecular wires based on phenylenevinylene oligomers: a quantum–chemical insight, J. Am. Chem. Soc. 124 (2002) 4436–4447.
[90] B. Giese, S. Wessely, M. Spormann, U. Lindemann, E. Meggers, M.E. Michel-Beyerle, On the mechanism of long-range electron-transfer through DNA, Angew. Chem., Int. Ed. Engl. 38 (1999) 996–998.
[91] E. Meggers, M.E. Michel-Beyerle, B. Giese, Sequence dependent long-range hole transport in DNA, J. Am. Chem. Soc. 120 (1998) 12950–12955.
[92] M. Bixon, B. Giese, S. Wessely, T. Langenbacher, M.E. Michel-Beyerle, J. Jortner, Long-range charge hopping in DNA, Proc. Natl. Acad. Sci. U.S.A. 96 (1999) 11713–11716.
[93] M. Bixon, J. Jortner, Electron-transfer—from isolated molecules to biomolecules, Adv. Chem. Phys. 106 (1999) 35–202.
[94] Y.A. Berlin, A.L. Burin, M.A. Ratner, Charge hopping in DNA, J. Am. Chem. Soc. 123 (2001) 260–268.
[95] Y.A. Berlin, A.L. Burin, M.A. Ratner, On long-range charge transfer in DNA, J. Phys. Chem. A 104 (2000) 443–445.
[96] J.R. Reimers, N.S. Hush, Electronic properties of transition-metal complexes determined from electro-absorption (Stark) spectroscopy. 2. Mononuclear complexes of ruthenium(II), J. Phys. Chem. 95 (1991) 9773–9781.
[97] N.S. Hush, Adiabatic theory of outer-sphere electron-transfer reactions in solution, Trans. Faraday Soc. 57 (1961) 557–580.
[98] N.S. Hush, Homogeneous and heterogeneous optical and thermal electron-transfer, Electrochim. Acta 13 (1968) 1005–1023.
[99] N.S. Hush, Intervalence-charge transfer absorption. II. Theoretical considerations and spectroscopic data, Prog. Inorg. Chem. 8 (1967) 391–444.
[100] R.S. Mulliken, Molecular complexes and their spectra: part II, J. Am. Chem. Soc. 64 (1952) 811–824.
[101] R.J. Cave, M.D. Newton, Generalization of the Mulliken–Hush treatment for the calculation of electron-transfer matrix elements, Chem. Phys. Lett. 249 (1996) 15–19.
[102] E. Cukier, S. Daniels, E. Vinson, R.J. Cave, Are hydrogen bonds unique among weak interactions in their ability to mediate electronic coupling? J. Phys. Chem. A 106 (2002) 11247–11340.
[103] M. Rust, J. Lappe, R.J. Cave, Multi-state effects in calculations of the electronic coupling element for electron-transfer using the generalised Mulliken–Hush method, J. Phys. Chem. A 106 (2002) 3930–3940.
[104] C.M. Elliott, D.L. Derr, D.V. Matyushov, M.D. Newton, Direct experimental comparison of the theories of thermal and optical electron-transfer: studies of a mixed-valence dinuclear iron polypyridyl complex, J. Am. Chem. Soc. 120 (1998) 11714–11726.
[105] S. Hayashi, S. Kato, Theoretical study of intramolecular long-range electron-transfer reactions between porphyrin and benzoquinone: ab initio calculation of the electronic coupling matrix element, J. Phys. Chem. 102 (1998) 2878–2887.
[106] Y.Q. Gao, R.A. Marcus, Theoretical investigation of the directional electron-transfer in 4-aminonaphthalimide compounds, J. Phys. Chem. A 106 (2002) 1956–1960.
[107] I. Daizadeh, J.N. Gehlen, A.A. Stuchebrukhov, Calculation of the electronic tunnelling matrix element in proteins: comparison of exact and approximate one-electron methods for Ru-modified azurin, J. Chem. Phys. 106 (1997) 5658–5666.
[108] A.H.A. Clayton, K.P. Ghiggino, G.J. Wilson, M.N. Paddon-Row, Semi-empirical investigation of charge-transfer interactions in rigid dimethoxynaphthalene–bridge–pyridinium systems, J. Phys. Chem. 97 (1993) 7962–7969.
[109] D.J. Katz, A.A. Stuchebrukhov, Calculation of electronic tunnelling matrix element in proteins: comparison of exact and approximate one-electron methods for Ru-modified azurin, J. Chem. Phys. 106 (1997) 5658–5666.
[110] A. Voityuk, J. Jortner, M. Bixon, N. Rösch, Electronic coupling between Watson–Crick pairs for hole transfer and transport in deoxyribonucleic acid, J. Chem. Phys. B 114 (2001) 5614–5620.
[111] A.A. Voityuk, N. Rösch, M. Bixon, J. Jortner, Electronic coupling for charge transfer and transport in DNA, J. Phys. Chem. B 104 (2000) 9740–9745.
[112] S. Steenken, Purine bases, nucleosides, and nucleotides: aqueous solution redox chemistry and transformation reactions of their radical cations and e- and OH adducts, Chem. Rev. 89 (1987) 503–520.
[113] P.J. Dandliker, R.E. Holmin, J.K. Barton, Oxidative thymine dimer repair in the DNA helix, Science 75 (1997) 1465–1468.
[114] J. Jortner, M. Bixon, T. Langenbacher, M.E. Michel-Beyerle, Charge transfer and transport in DNA, Proc. Natl. Acad. Sci. U.S.A. 95 (1998) 12759–12765.
[115] D. Ly, Y. Kan, B. Armitage, G.B. Schuster, Cleavage of DNA by irradiation of substituted anthraquinones: intercalation promotes electron-transfer and efficient reaction at GG steps, J. Am. Chem. Soc. 118 (1996) 8747–8748.
[116] H. Sugiyama, I. Saito, Theoretical studies of GG-specific photocleavage of DNA via electron-transfer: significant lowering of ionization potential and 5′-localization of HOMO of stacked GG bases in B-form DNA, J. Am. Chem. Soc. 118 (1996) 7063–7068.
[117] I. Saito, T. Nakamura, K. Nakatani, Y. Yoshioka, K. Yamaguchi, H. Sugiyama, Mapping of the hot spots for DNA damage by one-electron oxidation: efficacy of GG doublets and GGG triplets as a trap in long-range hole migration, J. Am. Chem. Soc. 120 (1998) 12686–12687.
[118] F. Prat, K.N. Houk, C.S. Foote, Effect of guanine stacking on the oxidation of 8-oxoguanine in B-DNA, J. Am. Chem. Soc. 120 (1998) 845–846.
[119] S. Steenken, Electron-transfer in DNA. Competition by ultra-fast proton transfer, Biol. Chem. 378 (1997) 1293–1297.
[120] D.N. Beratan, J.N. Betts, J.N. Onuchic, Tunnelling pathways and redox-state dependent electronic coupling at nearly fixed distance in electron-transfer proteins, J. Phys. Chem. 96 (1992) 2852–2855.
[121] D.N. Beratan, J.N. Onuchic, J.J. Hopfield, Electron tunnelling through covalent and non-covalent pathways in proteins, J. Chem. Phys. 86 (1987) 4488–4498.
[122] D.N. Beratan, J.N. Onuchic, J.N. Betts, B.E. Bowler, H.B. Gray, Electron-tunnelling pathways in ruthenated proteins, J. Am. Chem. Soc. 112 (1990) 7915–7921.
[123] D.N. Beratan, J.N. Onuchic, Electron-tunnelling pathways in proteins: influences on the transfer rate, Photosynth. Res. 22 (1989) 173–186.
[124] J.N. Betts, D.N. Beratan, J.N. Onuchic, Mapping electron tunnelling pathways: an algorithm that finds the “minimum length”/maximum coupling pathway between electronic donors and acceptors in proteins, J. Am. Chem. Soc. 114 (1992) 4043–4046.
[125] J.N. Onuchic, D.N. Beratan, A predictive theoretical model for electron tunnelling pathways in proteins, J. Chem. Phys. 92 (1990) 722–733.
[126] J.J. Regan, S.M. Risser, D.N. Beratan, J.N. Onuchic, Protein electron transport: single versus multiple pathways, J. Phys. Chem. 97 (1993) 13083–13088.
[127] G.M. Ullmann, N.M. Kostiæ, Electron-tunnelling paths in various electrostatic complexes between cytochrome *c* and plastocyanin. Anisotropy of the copper–ligand interactions and dependence of the iron–copper electronic coupling on the metallo-protein orientation, J. Am. Chem. Soc. 117 (1995) 4766–4774.
[128] J.C. Tully, B. Bunsen-Ges, Trajectories in ion–molecule reactions, J. Phys. Chem. 77 (1973) 557–565.
[129] J.C. Tully, in: W.H. Miller (Ed.), Dynamics of Molecular Collisions, Part B, Plenum Press, New York, 1976, p. 217.
[130] J.C. Tully, R.K. Preston, Trajectory surface hopping approach to non-adiabatic molecular collisions. Reaction of H^+ with molecular deuterium, J. Chem. Phys. 55 (1971) 562–572.

[131] W.H. Miller, T.F. George, Semi-classical theory of electronic transitions in low-energy atomic and molecular collisions involving several nuclear degrees of freedom, J. Chem. Phys. 56 (1972) 5637–5652.
[132] J.R. Stine, J.T. Muckerman, On the multi-dimensional surface intersection problem and classical trajectory "surface hopping", J. Chem. Phys. 65 (1976) 3975–3984.
[133] G.A. Jones, B.K. Carpenter, M.N. Paddon-Row, Application of trajectory surface hopping to the study of intramolecular electron-transfer in polyatomic organic systems, J. Am. Chem. Soc. 120 (1998) 5499–5508.
[134] C. Zerner, Non-adiabatic crossing of energy levels, Proc. R. Soc. London, Ser. A 137 (1932) 696.
[135] L.D. Landau, E.M. Lifshitz, Quantum Mechanics, Pergamon Press, New York, 1962.
[136] L.D. Landau, Zur Theorie der Energieubertragung I, Z. Sowjetunion 1 (1932) 88–95.
[137] L.D. Landau, Zur Theorie der Energieubertragung II, Z. Sowjetunion 2 (1932) 46–51.
[138] G.A. Jones, B.K. Carpenter, M.N. Paddon-Row, Application of trajectory surface hopping to the study of a symmetry-forbidden intramolecular hole transfer process in bismethyleneadamantane cation radical, J. Am. Chem. Soc. 121 (1999) 11171–11178.
[139] J.J.P. Stewart, L.P. Davis, L.W. Burggraf, Semi-empirical calculations of molecular trajectories: method and applications to some simple molecular systems, J. Comput. Chem. 8 (1987) 1117–1123.

Professor Anthony Harriman spent 14 years at the Royal Institution of Great Britain in London, working with Lord George Porter. He moved to the University of Texas at Austin in 1988 to become Director of the Center for Fast Kinetics Research. In 1995, he moved to the Universite Louis Pasteur in Strasbourg, France before moving to the University of Newcastle in 1999. He research interests involve artificial photosynthesis and molecular photonics.

Ata Amini was born in Iran. He received his BSc and MSc in chemistry from Isfahan and Shiraz Universities, respectively, and he will receive his PhD from the University of Newcastle in October 2003. His main research interest over the past few years concerns the use of modern computational chemistry techniques for the investigation of the rate of electron-transfer in organic, inorganic and macromolecules. He is particularly interested in the use of quantum chemical approaches for solving problems related to biological molecules, such as metallo-proteins.